REPORT DOCUMENTATION PAGE

1. REPORT DATE (DD-MM-YYYY)	2. REPORT TYPE	3. DATES COVERED (From - To)
2002	Journal Article	

4. TITLE AND SUBTITLE	5a. CONTRACT NUMBER
Bioluminescence flow visualization in the ocean: an initial strategy based on laboratory experiments	5b. GRANT NUMBER
	5c. PROGRAM ELEMENT NUMBER

6. AUTHORS	5d. PROJECT NUMBER
Jim Rohr, Stewart Fallon[1]	
Mark Hyman[2]	5e. TASK NUMBER
Michael I. Latz[3]	5f. WORK UNIT NUMBER

7. PERFORMING ORGANIZATION NAME(S) AND ADDRESS(ES)

[1]SSC San Diego
53560 Hull Street
San Diego, CA 92152-5001

[2]Coastal Systems Station
Code R11
Panama City, FL
32407-7001

[3]Scripps Institute of
Oceanography, UCSD
9500 Gilman Drive
La Jolla, CA 92093-0202

8. PERFORMING ORGANIZATION REPORT NUMBER

9. SPONSORING/MONITORING AGENCY NAME(S) AND ADDRESS(ES)

10. SPONSOR/MONITOR'S ACRONYM(S)

11. SPONSOR/MONITOR'S REPORT NUMBER(S)

12. DISTRIBUTION/AVAILABILITY STATEMENT
Approved for public release; distribution is unlimited.

13. SUPPLEMENTARY NOTES
This is the work of the United States Government and therefore is not copyrighted. This work may be copied and disseminated without restriction. Many SSC San Diego public release documents are available in electronic format at: http://www.spawar.navy.mil/sti/publications/pubs/index.html

14. ABSTRACT
Observations of flow-stimulated bioluminescence have been recorded for centuries throughout the world's oceans. The present study explores, within a laboratory context, the use of naturally occurring bioluminescence as a strategy towards visualizing oceanic flow fields. The response of luminescent plankton to quantifiable levels of flow agitation was investigated in fully developed pipe flow. With two different pipe flow apparatus and freshly collected mixed plankton samples obtained over a year at two separate locations, several repeatable response patterns were identified. Threshold levels for bioluminescence stimulation occurred in laminar flow with wall shear stress levels generally between 1 and 2 dyn cm^{-2} (0.1–0.2 N m^{-2}), equivalent to energy dissipation per unit mass values of 10^2–10^3 cm^{2}s^{-3} (10^{-2}–10^{-1}m^{2}s^{-3}). In an attempt to account for different concentrations and assemblages of mixed plankton, mean bioluminescence levels were normalized by an index of the corresponding flow-stimulated bioluminescence potential. This procedure generally accounted for variability between turbulent flow experiments, but was not effective for laminar flow. In turbulent flow, mean bioluminescence levels increased approximately linearly with wall shear stress. The magnitude of the flash response of individual cells, however, remained nearly constant throughout high laminar and turbulent flow, even as the energetic length scales of the turbulence became less than the size of the organisms of interest. Threshold flow stimuli levels determined in the laboratory were compared with oceanic measurements taken from the literature and with numerical simulations of ship wakes, one of the few highy turbulent flows to be well studied. Several oceanic flow fields are proposed as candidates for bioluminescence flow visualization.
Published in *Deep-Sea Research Part I*. Volume 49, pp. 2009–2033, 2002.

15. SUBJECT TERMS

Bioluminescence	Laminar flow
Dinoflagellate	Ship wake simulation
Flow visualization	Turbulent flow

16. SECURITY CLASSIFICATION OF:			17. LIMITATION OF ABSTRACT	18. NUMBER OF PAGES	19a. NAME OF RESPONSIBLE PERSON
a. REPORT	b. ABSTRACT	c. THIS PAGE			Jim Rohr, Code 2112
U	U	U	UU	25	19B. TELEPHONE NUMBER (Include area code) (619) 553-1604

Bioluminescence flow visualization in the ocean: an initial strategy based on laboratory experiments

Jim Rohr[a], Mark Hyman[b], Stewart Fallon[a,1], Michael I. Latz[c,*]

[a] SSC San Diego, 53560 Hull Street, D363, San Diego, CA 92152, USA
[b] Coastal Systems Station, Code R11, Panama City, FL 32407-7001, USA
[c] Scripps Institution of Oceanography, University of California San Diego, 9500 Gilman Drive, La Jolla, CA 92093-0202, USA

Abstract

Observations of flow-stimulated bioluminescence have been recorded for centuries throughout the world's oceans. The present study explores, within a laboratory context, the use of naturally occurring bioluminescence as a strategy towards visualizing oceanic flow fields. The response of luminescent plankton to quantifiable levels of flow agitation was investigated in fully developed pipe flow. With two different pipe flow apparatus and freshly collected mixed plankton samples obtained over a year at two separate locations, several repeatable response patterns were identified. Threshold levels for bioluminescence stimulation occurred in laminar flow with wall shear stress levels generally between 1 and 2 $dyn\,cm^{-2}$ (0.1–0.2 $N\,m^{-2}$), equivalent to energy dissipation per unit mass values of 10^2–$10^3\,cm^2\,s^{-3}$ (10^{-2}–$10^{-1}\,m^2\,s^{-3}$). In an attempt to account for different concentrations and assemblages of mixed plankton, mean bioluminescence levels were normalized by an index of the corresponding flow-stimulated bioluminescence potential. This procedure generally accounted for variability between turbulent flow experiments, but was not effective for laminar flow. In turbulent flow, mean bioluminescence levels increased approximately linearly with wall shear stress. The magnitude of the flash response of individual cells, however, remained nearly constant throughout high laminar and turbulent flow, even as the energetic length scales of the turbulence became less than the size of the organisms of interest. Threshold flow stimuli levels determined in the laboratory were compared with oceanic measurements taken from the literature and with numerical simulations of ship wakes, one of the few highly turbulent flows to be well studied. Several oceanic flow fields are proposed as candidates for bioluminescence flow visualization.
Published by Elsevier Science Ltd.

Keywords: Bioluminescence; Dinoflagellate; Flow visualization; Laminar flow; Ship wake simulation; Turbulent flow; USA; California; San Diego Bay; Scripps Institution of Oceanography Pier

1. Introduction

1.1. Motivation

There is no doubt that ship wakes can produce spectacular displays of bioluminescence (Harvey, 1952, 1957; Tarasov, 1956; Staples, 1966).

*Corresponding author. Tel.: +1-858-534-6579; fax: +1-858-534-7313.
E-mail address: mlatz@ucsd.edu (M.I. Latz).
[1] Present address: Lawrence Livermore National Laboratory, Center for Accelerometer Mass Spectrometry, L-397 7000 East Avenue, Livermore, CA 94550, USA.

However, bioluminescence is also stimulated by much less energetic flows such as swell over submerged bodies (Rohr et al., 1994), swimming dolphins (Rohr et al., 1998), seals (Williams and Kooyman, 1985), small fish (Harvey, 1952), and divers (Lythgoe, 1972; Robinson, 1998). These observations suggest that several energetic geophysical flow fields may also be candidates for bioluminescence flow visualization. Through determination of bioluminescence threshold levels in well-characterized laboratory flow fields, geophysical flow fields that are likely candidates for bioluminescence flow visualization can begin to be assessed within a scientific context.

1.2. Background

Bioluminescence is one of the most cosmopolitan organism behaviors in the marine environment, having been found at all depths and in all oceans of the world (Clark and Denton, 1962; Widder, 1997). In coastal waters, where opportunities to observe flow-stimulated bioluminescence are typically best, the primary sources of bioluminescence are unicellular plankton called dinoflagellates (e.g., Seliger et al., 1961; Kelly and Tett, 1978; Morin, 1983; Lapota, 1998). It has been postulated that concentrations <100 dinoflagellates l^{-1} are sufficient to highlight moving objects (Morin, 1983) and that visual predators use flow-stimulated bioluminescence at night to locate their prey (Hobson, 1966; Mensinger and Case, 1992; Fleisher and Case, 1995). Where extended monitoring of coastal bioluminescence has been conducted, abundances of bioluminescent dinoflagellates were equal to or greater than 100 cells l^{-1} (Kelly, 1968; Lapota, 1998; Rapoport and Latz, 1998). During red tides, the abundance of luminescent dinoflagellates may reach 10^7 cells l^{-1} (Seliger et al., 1970). Thus, it appears that sufficient concentrations of bioluminescent dinoflagellates occur frequently enough in coastal waters to provide opportunities, when it is suitably dark, for nighttime oceanic flow visualization.

Some dinoflagellates are known to be very shear sensitive (Thomas and Gibson, 1990a, b; Estrada and Berdalet, 1997; Juhl et al., 2000; Zirbel et al., 2000). Generally, the shear sensitivity of animal

and plant cells is dependent on the length scales of the turbulence (reviewed by Hua et al., 1993). Shear stress (viscous) and turbulent length and time scales are also considered important parameters for bioluminescence stimulation (Anderson et al., 1988; Widder et al., 1993; Latz et al., 1994; Rohr et al., 1997). An experimental approach using fully developed pipe flow allows all these flow parameters to be examined. Fully developed pipe flow is also advantageous because: it offers a wide range of laminar and turbulent flow stimuli, organisms experience the flow field for only a brief time period and are continuously replaced, and significant depletion of bioluminescence does not occur in the upstream length of pipe (Losee and Lapota, 1981; Rohr et al., 1994).

Bioluminescence response patterns for mixed plankton samples (Rohr et al., 1997) and laboratory cultures of the red-tide dinoflagellate *Lingulodinium polyedrum* (Latz and Rohr, 1999) have been reported as a function of pipe wall shear stress, τ_{wall}, for predominantly laminar flows. The present study examined the repeatability of these response patterns by testing freshly collected mixed plankton at two different locations over a year with the same pipe flow apparatus and experimental approach. Because only a small range of turbulent flow has been previously investigated (Rohr et al., 1997; Latz and Rohr, 1999), the effect of length and time scales of the turbulence on flow-stimulated dinoflagellate bioluminescence is not known. The present study also used a larger pipe flow apparatus to obtain a greater range of turbulent length and time scales. Throughout these experiments the homogeneity of mixed plankton abundance was assessed by periodic measurement of an index of the bioluminescence potential. These measurements provided an opportunity to investigate whether mean bioluminescence measurements obtained for different mixed plankton assemblages, but for the same flow stimuli, could be effectively scaled with an index of bioluminescence potential.

Another important hydrodynamic feature is the rate of energy dissipation per unit mass, hereafter referred to as the dissipation, ε. Together with the kinematic viscosity, dissipation determines the Kolmogorov scales which are indicative of

the smallest length, L_K, and time, L_T, scales of the turbulence. At small scales, instantaneous shear stress and dissipation are different descriptors of the same flow phenomenon, the deformation of the fluid. The relationship between τ and ε depends on the flow field and author's preference, but has a common form:

$$\varepsilon = k(\tau)^2(\nu\rho^2)^{-1}, \tag{1}$$

where ν and ρ are the kinematic viscosity and density of seawater, respectively, and k is a constant. For mathematical convenience k often appears as 2π in the oceanic literature (Mann and Denny, 1996). In fully developed laminar pipe flow, k is indisputably, equal to one (Rosenhead, 1963; Sherman, 1990). Assuming $k = 1$, Eq. (1) has been used to study the effect of wind-induced turbulence on dinoflagellate population growth (Thomas and Gibson, 1990a), surf-zone turbulence on purple sea urchin fertilization (Mead and Denny, 1995), and the biological consequences of small-scale flow in a surge channel (Denny et al., 1992). A similar expression, but with k equal to $10/\pi$, has been employed by Latz et al. (1994) to estimate oceanic bioluminescence threshold dissipation levels, using threshold shear stress values determined in simple laminar Couette flow. Lazier and Mann (1989) suggest, based on the velocity shear spectra measured in a mixed layer (Oakey and Elliot, 1980), that for most turbulent oceanographic applications $k = 7.5$. For the present oceanic comparisons a range of dissipation threshold levels was calculated from threshold shear stress values determined in laminar pipe flow, Eq. (1), and k values of 1 and 7.5. Although threshold dissipation and threshold shear stress values are not independent measurements, in the present study they are considered separately when compared to oceanographic shear and dissipation measurements.

2. Experimental materials and methods

2.1. Pipe flow measurements

The smaller pipe flow apparatus used in this study was identical to that described by Rohr et al.

(1997) and Latz and Rohr (1999). It consisted of a 91-cm long, 0.64-cm inner diameter (i.d.), transparent acrylic pipe connected to a 75-l head tank. A manual valve at the end of the pipe controlled the flow. Mean flow speeds up to $2.4\,\mathrm{m\,s^{-1}}$ were achieved, providing maximum levels of viscous stress at the pipe wall (τ_{wall}) of about $220\,\mathrm{dyn\,cm^{-2}}$ ($= 22\,\mathrm{N\,m^{-2}}$) (Table 1). The 0.64-cm i.d. pipe flow apparatus was used to investigate the response of freshly collected plankton samples obtained from San Diego (SD) Bay and off the Scripps Institution of Oceanography (SIO) Pier, La Jolla, CA. Between 30 May, 1994 and 11 July, 1995, six 0.64-cm i.d. pipe flow experiments with mixed plankton samples were performed at each location (Table 2).

To obtain higher shear stresses, a pressurized pipe flow apparatus incorporating a 450-l inertly coated stainless-steel head tank was assembled within an enclosure on a pier in SD Bay. Water was first drawn into a submerged tank through a 7.6-cm diameter, hydraulically actuated valve located 2–3 m below the sea surface. The submerged tank was then gradually pressurized to slowly transfer the water into the head tank. The maximum shear stress during transport through the 10-cm i.d. connecting hose was estimated as less than $1\,\mathrm{dyn\,cm^{-2}}$. Mounted to the bottom of the head tank was a 50-cm-diameter elbow connected to a flange from which issued a 3-m long, clear acrylic pipe of 0.85-cm i.d. Between the pipe and the flange was a smooth contracting inlet with a cubic polynomial profile. Through pressurizing the head tank and controlling a manual valve at the end of the pipe, flow speeds in excess of $6\,\mathrm{m\,s^{-1}}$, with associated maximum τ_{wall} levels around $1000\,\mathrm{dyn\,cm^{-2}}$, were attained (Table 1). Six experiments were successfully conducted between 28 April, 1994 and 18 August, 1994 in the 0.85-cm i.d. pipe (Table 2). For comparison, an overlapping range of τ_{wall} values was measured for both pipes. Each experiment for either apparatus consisted of a single tank full of freshly collected seawater.

Pressure drop, Δp, between the pressure taps separated by Δx along the pipe, was measured with variable reluctance differential transducers (Validyne Corporation). Mean flow speed, U_{avg}, was calculated by dividing the volume flow rate by the

Table 1

Range of wall shear stress, τ_{wall}, energy dissipation per unit mass, ε, and Kolmogorov length, L_K, and time, L_T, scales (at centerline, $L_{Kc/l}$, $L_{Tc/l}$; averaged across the pipe diameter, L_{Kavg}, L_{Tavg}; and at the pipe wall, L_{Kwall}, L_{Twall}) for the pipe flow experiments

Pipe i.d. (cm)	Laminar flow		Turbulent flow							
	τ_{wall} (dyn cm^{-2})	ε_{wall} (cm^2 s^{-3})	τ_{wall} (dyn cm^{-2})	ε_{wall} ($\times 10^6$ cm^2 s^{-3})	$L_{Kc/l}$ (μm)	L_{Kavg} (μm)	L_{Kwall} (μm)	$L_{Tc/l}$ (μs)	L_{Tavg} (μs)	L_{Twall} (μs)
0.64	0.2–29	3.6–76000	61–220	0.3–4.3	25–14	22–13	14–7	610–190	470–170	180–49
0.85	0.3–8	8.2–5800	20–1000	0.03–91	44–8	37–8	25–3	1800–26	1300–30	570–11

Table 2

Mixed plankton, bioluminescence pipe flow results. Mean slope is based on the least-squares regression of log mean bioluminescence vs. log τ_{wall}, with number of measurements in parentheses and r^2 values in brackets

Experiment	Threshold τ_{wall} (dyn cm^{-2})	Mean slope	
Location and date		Laminar	Turbulent
SD Bay 0.64-cm i.d.			
5/30/94	1.4	2.1 (18) [0.97]	
6/02/94	1.1	1.8 (14) [0.96]	
7/06/95	1.3	2.1 (13) [0.99]	
7/07/95	1.1	1.8 (20) [0.98]	
7/11/95	1.1	1.4 (13) [0.93]	
7/18/95	1.7	2.0 (14) [0.97]	
Pooled data	1.3±0.26	1.9±0.28	
SIO Pier 0.64-cm i.d.			
7/11/94	0.9	1.8 (13) [0.96]	
7/13/94	0.6	1.3 (10) [0.83]	
8/08/94	0.7	1.5 (9) [0.95]	
9/07/94	0.7	1.7 (21) [0.94]	
4/14/95	1.2	2.2 (27) [0.93]	
4/27/95	1.2	2.2 (22) [0.93]	
Pooled data	0.9±0.25	1.8±0.34	
SD Bay 0.85-cm i.d. Spring 1994			
4/28/94	1.2	2.5 (8) [0.94]	0.9 (10) [0.96]
5/01/94	0.7	2.1 (12) [0.95]	0.9 (17) [0.96]
5/09/94	0.7	1.7 (9) [0.76]	1.3 (28) [0.98]
5/10/94	0.6	1.9 (12) [0.76]	1.2 (13) [0.93]
Pooled data	0.8±0.25	2.0±0.37	1.1±0.21
SD Bay 0.85-cm i.d. Summer 1994			
7/27/94	0.8	1.7 (8) [0.66]	1.1 (14) [0.93]
8/18/94	1.0	2.0 (5) [0.99]	0.9 (06) [0.98]
Pooled data	0.9±0.16	1.9±0.20	1.0±0.19

pipe cross-sectional area. The volume flow rate was determined by weighing the flow discharge collected over a measured time. Darcy friction factor, a dimensionless pressure, and Reynolds number, a dimensionless flow rate, were calculated (Schlichting, 1979) for each bioluminescence measurement as previously described (Latz and Rohr, 1999). Their relationship clearly marks where the
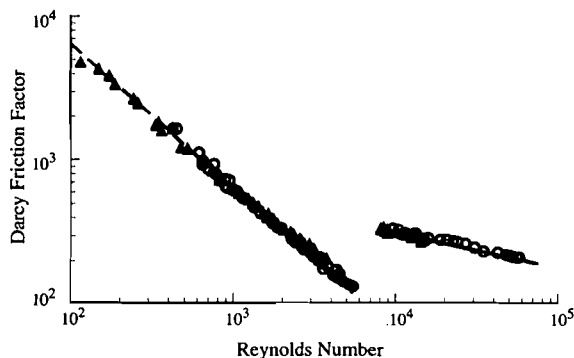
Fig. 1. Representative measurements of Darcy friction factor and Reynolds number. The dashed line is the theoretical relationship for laminar flow; the solid line is the accepted empirical relationship for turbulent flow (Schlichting, 1979). Closed traingles are data collected from the 0.64-cm i.d. pipe; open circles are data collected from the 0.85-cm i.d. pipe.

flow was laminar, turbulent, or transitional, and whether the measurements were obtained in fully developed pipe flow. The break between the data (Fig. 1) represents the region of transition from laminar to turbulent flow.

The shear stress in fully developed pipe flow, regardless of whether the flow is laminar or turbulent, increases linearly from zero at centerline to a maximum at the pipe wall (Schlichting, 1979). The wall shear stress in fully developed pipe flow is directly calculated from either measurements of pressure drop or average flow rate (Schlichting, 1979).

In turbulent pipe flow, ε decreases rapidly with distance from the pipe wall (Laufer, 1954). Estimates of ε at the pipe wall (Eq. (1); $k = 1$), centerline (Davies, 1972), and averaged across the pipe (Bakhmeteff, 1936) were made, and the corresponding values of the Kolmogorov length (L_{Kwall}, $L_{\text{Kc/l}}$, L_{Kavg}) and time (L_{Twall}, $L_{\text{Tc/l}}$, L_{Tavg}) scales were calculated (Tennekes and Lumley, 1972). Kolmogorov length and time scales varied between 1 (3–39 μm) and 2 (11–1300 μs) orders of magnitude, respectively (Table 1).

2.2. Luminescent organisms

The luminescent organisms identified in the pipe flow samples obtained throughout this study were exclusively dinoflagellates, primarily *L. polyedrum*

(formerly *Gonyaulax polyedra*; 40 μm in diameter), *Ceratium fusus* (340 × 30 μm, length and width, respectively) and *Protoperidinium* spp. (70 × 60 μm). When mechanically stimulated until bioluminescence is depleted, *L. polyedrum*, *C. fusus* and *Protoperidinium* spp. produce 1–2 × 10^8 (Biggley et al., 1969; Latz and Lee, 1995), 3–5 × 10^8 (Esaias et al., 1973; Sullivan and Swift, 1994) and 0.5–3 × 10^9 (Lapota et al., 1989; Swift et al., 1995) photons cell⁻¹, respectively.

These particular luminescent dinoflagellates are common to the coastal waters off · southern California (e.g., Sweeney, 1963; Holmes et al., 1967; Kimor, 1983; Lapota, 1998). Although the most abundant dinoflagellate, *L. polyedrum*, is motile (Kamykowski et al., 1992), its swimming is weak compared to the flows considered throughout this study. Like most bioluminescent dinoflagellates, *L. polyedrum* exhibits a circadian rhythmicity with emission one to two orders of magnitude greater at night than during the day (Biggley et al., 1969; Sweeney, 1981). Dinoflagellates typically respond to mechanical stimulation within 20 ms with a light flash of 100 ms or more in duration (Eckert, 1965; Widder and Case, 1981; Latz and Lee, 1995).

For the 0.64-cm i.d. pipe flow experiments, surface seawater was collected by bucket from SD Bay and off the SIO Pier, 2 h before sunset when dinoflagellate bioluminescence is minimally excitable (Biggley et al., 1969). At dusk, the apparatus was covered with opaque sheeting and experiments commenced 2.5 h later, when maximal levels of bioluminescence are expected (Biggley et al., 1969). For the 0.85-cm i.d. pipe flow experiments, the organisms were drawn from an underwater reservoir 2 h before sunset and were immediately introduced into an opaque head tank. Measurements commenced 2.5 h after sunset.

2.3. Bioluminescence measurements

Bioluminescence was measured with photon-counting photomultiplier (PMT) detectors as described by Latz and Rohr (1999). Mean bioluminescence was calculated by averaging each data record and was expressed as counts s⁻¹. PMT pulses were also counted in 5-ms time bins to

resolve individual flash events. Maximum biolu-
minescence was determined by taking the highest
5-ms integration value in each time series and was
expressed as counts $5\,ms^{-1}$. Maximum biolumi-
nescence measurements serve as an indicator of the
peak intensity of an individual flash (Rohr et al.,
1997; Latz and Rohr, 1999).

The same PMT was used for all the pipe flow
bioluminescence measurements, and was mounted
67 cm from the inlet of the 0.64-cm i.d. pipe and
2.36 m from the inlet of the 0.85-cm i.d. pipe. The
PMT was coupled to the pipe with a light-shielded
adapter and viewed the entire pipe diameter and a
pipe length of 5 cm. A reference PMT, used for the
0.85-cm i.d. pipe flow experiments,' was mounted
to the quartz window opposite a 25.5-ml viewing
chamber of a flow agitator (described in Section
2.4). Simultaneous pipe flow bioluminescence
measurements obtained with both PMTs mounted
opposite to each other showed that their sensitiv-
ities were within a few percent. Each PMT record
was obtained at a constant flow rate, providing a
fixed τ_{wall} for periods typically between 20 and
100 s. The longer time series were collected for the
slower flow rates so that flow volumes for all the
time series were approximately equal. A sampling
duration of 100 s for the low flow rates was
adequate for detection of the response threshold
(Latz and Rohr, 1999). Neutral density filters were
used to attenuate the photon input to ensure that
bioluminescence was never saturating the PMT.

A response threshold was calculated for each
pipe flow experiment by a method similar to that
of Latz and Rohr (1999). First, for each of
the three pooled data sets (i.e., SIO Pier, 0.64-cm
i.d. pipe; SD Bay, 0.64-cm i.d. pipe; and SD Bay,
0.85-cm i.d. pipe) a range of laminar flows was
identified by eye, based on a trend for increasing
mean and maximum bioluminescence intensities
with increasing τ_{wall}. Then, for each of the pipe
flow experimental data sets, a least-squares regres-
sion of log mean bioluminescence vs. log wall
shear stress was calculated throughout this range.
Threshold τ_{wall} values were determined from this
regression equation to calculate where the regres-
sion line intercepted background mean biolumi-
nescence levels (Latz and Rohr, 1999). A
corresponding range of threshold dissipation

values were calculated by substituting threshold
τ_{wall} into Eq. (1) with $k = 1$ and 7.5.

Background mean bioluminescence levels were
measured with no flow and were composed of
electronic noise, ambient light leakage, and spon-
taneous bioluminescence (of which only the last
parameter will depend on cell concentration).
Mean and maximum background levels for
both PMT's were usually within 40–60 and
$10–30\,counts\,5\,ms^{-1}$, respectively, throughout all
the experiments. A representative mean back-
ground level of $45\,counts\,s^{-1}$ was chosen for
determining threshold τ_{wall} levels. Results ' were
largely insensitive, within a factor of 2, to the exact
choice of PMT background level.

For consistency, all bioluminescence measure-
ments were expressed as emission per time. This is
the most meaningful way to present response
threshold and maximum intensity. However,
measurements of flow-stimulated, mean biolumi-
nescence are often expressed as emission per
volume (Widder et al., 1993; Latz et al., 1994;
Widder, 1997). This particular representation
attempts to account for advective effects that are
most pronounced when the residency time of the
flash within the view of the detector is long
compared to its duration (Seliger et al., 1969;
Widder et al., 1993; Widder, 1997). Extending the
mathematical analysis for bathyphotometers (Se-
liger et al., 1969; Widder et al., 1993) to fully
developed pipe flow, Rohr et al. (1994) derived a
relationship between mean intensity, flash kinetics
and organism residency times. Applying this
analysis throughout the present range of τ_{wall} for
both the 0.64- and 0.85-cm i.d. pipe flow experi-
ments, an approximate linear dependence on
advection was found for both pipes. Consequently,
log mean bioluminescence vs. log τ_{wall} trends for
the 0.64- and 0.85-cm i.d. pipes can be directly
compared because the effect of advection is
similar. Least-squares regressions of log mean
bioluminescence vs. log τ_{wall} were used to calculate
slopes (mean $\pm$ standard deviation) and r^2 values.

2.4. Homogeneity and bioluminescence potential

The lack of homogeneity of bioluminescent
organisms throughout the head tank can have as

much, or more, of an effect on bioluminescence intensity as changes in the level of flow agitation. Through "gentle" pre-stirring of the 75-l head tank, differences in cell abundance between samples collected at the end of the 0.64-cm-diameter pipe were typically less than 30% throughout an experiment. Previous tests have shown that "gentle" pre-stirring, which did not stimulate bioluminescence, had no significant effect on the hydrodynamic agitation threshold for bioluminescence (Latz and Rohr, 1999). To test for cell homogeneity in the pre-stirred 75-l head tank, bioluminescence measurements were first collected for flow rates that proceeded in a decreasing sequence and then an overlapping, increasing sequence. An experiment was rejected only if similar flow rates did not produce similar bioluminescent intensities. Based on this criterion, all 12 pre-stirred, 0.64-cm i.d. pipe experiments were acceptable for further analysis.

The 450-l pressurized head tank, which could not be pre-stirred, was subject to larger fluctuations in cell concentration during an experiment. Therefore, in addition to comparing mean bioluminescence measurements for overlapping increasing and decreasing flow rates, an index of the flow-stimulated bioluminescence "potential" was measured periodically throughout each of the 0.85-cm i.d. pipe flow experiments. Bioluminescence potential indices were obtained with a flow agitator taken from a shipboard photometer system (Losee and Lapota, 1981; Losee et al., 1985; Lieberman et al., 1987). The flow agitator is composed of a 25.5-ml cylindrical chamber of 2.0-cm radius and 2.0-cm height, with quartz windows attached to its sides for viewing. The chamber's cylindrical axis is oriented perpendicular to the axis of the pipe. The inlet i.d. of the chamber reduces from 2.54 to 1 cm over a distance of 2.5 cm. The outlet from the chamber is a mirror image of the inlet. Because of the highly turbulent flow stimulus within the flow agitator, the associated bioluminescence measurements are assumed to serve as an effective index of the bioluminescence potential, i.e., the maximum bioluminescence intensity that can be hydrodynamically stimulated (Losee and Lapota, 1981; Losee et al., 1985; Lieberman et al., 1987). This presumption is partly corroborated by the fact that at sufficiently high flow rates, the details of the agitator chamber design (Losee et al., 1985), the length of upstream section preceding the agitator (Losee and Lapota, 1981), and the flow rate (Latz and Rohr, unpublished observations) do not significantly affect bioluminescence measurements within the agitator.

The flow agitator was attached to a 3.23-m length of 2.54-cm i.d. pipe, which ran parallel to the 0.85-cm i.d. pipe. Between the 2.54-cm i.d. pipe and the flange of the head tank was a smooth contracting inlet with the same cubic polynomial profile as the other pipes. The volume flow rate through the agitator was consistent with shipboard photometer protocol, always greater than $0.3 \, l \, s^{-1}$. Six of the nine 0.85 i.d. pipe flow tests conducted satisfied both criteria of repeatability for increasing and decreasing flow rates and approximately constant bioluminescence potential index throughout the experiment. These six experiments were further analyzed.

3. Computational methods

Some of the most comprehensive numerical simulations presently available for highly energetic flow fields in the ocean are for the wakes of naval ships (Rood, 1995). The objective of the present study was not to use bioluminescence to detect ship wakes per se, but to demonstrate how luminescent "footprints" could be predicted in turbulent oceanic flows. As numerical simulations evolve, bioluminescence associated with highly energetic geophysical flows can be estimated.

Numerical simulations were used to estimate the temporally and spatially averaged turbulent shear stress and energy dissipation fields throughout the wake of an aircraft carrier. These computations were then used to delineate where within the wake several candidate threshold values of turbulent shear stress and energy dissipation were attained or exceeded. The simulated aircraft carrier had four 6.4-m diameter propellers, a displacement of 9.1×10^4 tons, and at waterline a length, beam and draft of 332.5, 40.2 and 11 m, respectively. The simulation was for a typical speed of $9 \, m \, s^{-1}$, about 18 knots.

The algorithm used to compute the wake flow field, a parabolic Reynolds-averaged Navier–Stokes solver, is well-documented and has been partially verified with full-scale experiments on many classes of US naval surface craft (Hyman, 1990, 1992, 1994). For this initial assessment of ship wake bioluminescence signatures, the effect of rising bubbles on modifying the flow field was ignored. Because rising bubbles can stimulate luminescent plankton (Anderson et al., 1988; Latz and Case, unpublished observations), the bioluminescent "footprints" predicted by the present simulations are thought to be conservative.

Note that the turbulent or Reynolds shear stress calculated in the numerical simulations is fundamentally different than the threshold shear stress determined in laminar pipe flow. The turbulent length scales that dominate the Reynolds stresses tend to be the larger length scales of the flow (Stacey et al., 1999b). The smallest length scales in the simulations are many orders of magnitude greater than the bioluminescent dinoflagellates of interest. The distance between grid points varied from tens of centimeters at the free surface and centerline to tens of meters at the subsurface edges of the wake.

In principle, for large Reynolds number flows such as full-scale ship wakes, dissipation at the scales of luminescent plankton can be reliably discerned from measurements at much larger scales (Tritton, 1988). Unfortunately, except for a Direct Numerical Simulation, dissipation is the computed quantity with the largest uncertainty. Because there are no direct measurements of dissipation in a ship's wake, simulations must be checked indirectly, usually through another variable that is better understood and accurately measured. In the present case, the initial value of dissipation was derived from a length scale proportional to the propeller diameter, which was determined by optimizing the comparison of computations against a limited set of wake data taken in a tow tank (Swean, 1987). In subsequent simulations, while the near wake was fairly sensitive to dissipation error, most far-wake simulations were not, apparently tending towards a self-similar structure.

Irrespective of these difficulties, it is believed that the numerical simulation estimates of turbulent shear stress and energy dissipation are related to the local flow properties responsible for bioluminescence stimulation. The appropriate transfer functions can be derived given suitable field observations.

4. Experimental results

4.1. SD Bay and SIO Pier, 0.64-cm i.d. pipe flow bioluminescence measurements

Mean and maximum bioluminescence trends for the 0.64-cm i.d. pipe flow experiments with mixed plankton collected from SD Bay (six experiments) and off the SIO Pier (six experiments) were generally in good agreement (Fig. 2A and B; Table 2). With increasing laminar flow, mean and maximum bioluminescence normally increased above background levels in flows with τ_{wall} around $1\,dyn\,cm^{-2}$. For the range of $\tau_{wall} = 1{-}29\,dyn\,cm^{-2}$ in laminar flow, the increase in mean bioluminescence as the 1.9 ± 0.3 power of τ_{wall} for the six SD Bay experiments was not significantly different from the increase as the 1.8 ± 0.3 power for the six SIO Pier experiments ($t = 0.045$; d.f. $= 10$; $P = 0.66$). Pooling all laminar flow data for the two locations, mean bioluminescence increased as the 1.8 ± 0.3 power of τ_{wall} ($r^2 = 0.89$; $n = 194$). In turbulent flow, the relatively small logarithmic range of τ_{wall} between $62\,dyn\,cm^{-2}$ and $218\,dyn\,cm^{-2}$ and large scatter in the mean bioluminescence data precluded the identification of a meaningful power-law relationship.

Pooling all SD and SIO 0.64-cm i.d. pipe flow data from the two locations, the response threshold occurred in flows with a τ_{wall} of $1.1 \pm 0.3\,dyn\,cm^{-2}$. The corresponding τ_{wall} threshold values for the SD Bay and SIO Pier experiments were 1.3 ± 0.2 and $0.9 \pm 0.2\,dyn\,cm^{-2}$, respectively. Although as order of magnitude estimates these thresholds levels were remarkably similar, they were significantly different at the $P = 0.02$ level ($t = 2.746$; d.f. $= 10$). Comparing 1994 and 1995 measurements, there was no difference in
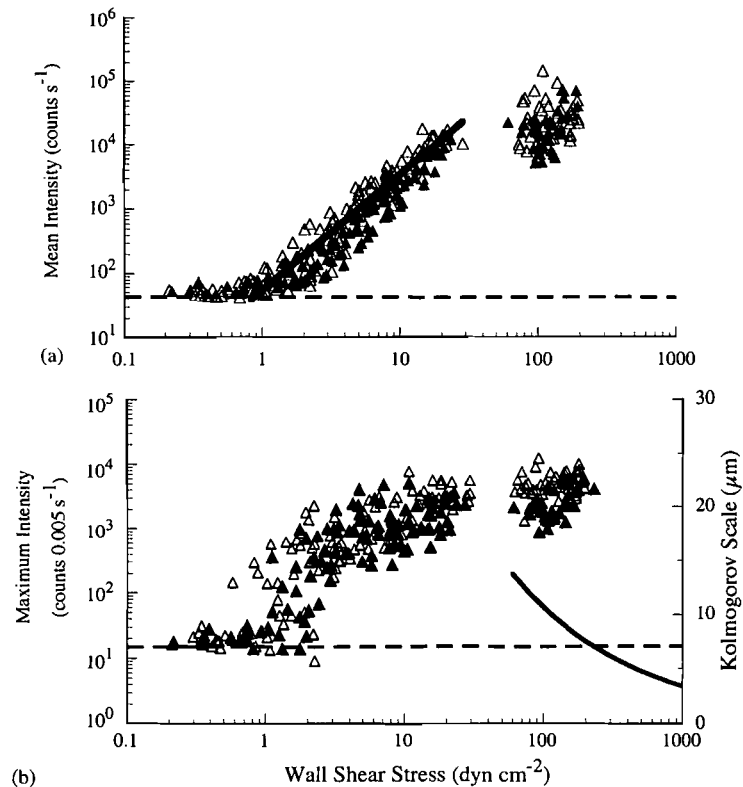
Fig. 2. Luminescent response of mixed plankton samples tested in the 0.64-cm i.d. pipe apparatus. Samples were collected from SD Bay (closed symbols) and SIO Pier (open triangles) over 1 year (Table 2). Each symbol indicates the result for one flow rate. Dashed lines represent the background level in the absence of flow. (A) Mean intensity as a function of wall shear stress. (B) Maximum intensity as a function of wall shear stress. The solid line indicates the Kolmogorov turbulent length scale, which is related to the smallest length scales of the turbulence. The smallest luminescent plankton present, *Lingulodinium polyedrum*, are about 40 μm in diameter. The gap in the data between τ_{wall} of 29–64 dyn cm^{-2} is the region where transition from laminar to turbulent flow occurred.

threshold τ_{wall} values for the two locations ($t = 0.471$; d.f. = 4; $P = 0.66$) in 1995, but in 1994 there was a significant difference ($t = 3.986$; d.f. = 4; $P = 0.02$) due to a lower threshold of 0.7 ± 0.1 dyn cm^{-2} at the SIO Pier location.

Maximum bioluminescence measurements exhibited greater variability than mean bioluminescence, particularly near threshold (Fig. 2B), because of the reduced statistical likelihood of observing the relatively short (≈ 10 ms) temporal peak of an individual flash. With increasing laminar flow, maximum bioluminescence measurements for all the 0.64-cm i.d. pipe flow experiments first increased more than two orders of magnitude between threshold and τ_{wall} values of 10 dyn cm^{-2}, and then remained nearly constant through transition from laminar to turbulent flow.

4.2. SD Bay, 0.85-cm i.d. pipe flow bioluminescence measurements

Throughout laminar flow, mean and maximum bioluminescence of SD Bay water samples tested in the 0.85-cm i.d. pipe apparatus increased as a function of τ_{wall} (Figs. 3A and B; Table 2) in a similar way as was found for the 0.64-cm i.d. pipe (Figs. 2A and B; Table 2). There was no significant difference in τ_{wall} threshold ($t = 0.471$; df = 4; $P = 0.66$) and mean slope ($t = 0.735$; d.f. = 4; $P = 0.50$) between spring and summer 1994 measurements in the 0.85-cm i.d. pipe. The bioluminescence stimulation threshold for the pooled data occurred in laminar flows with $\tau_{wall} = 0.8 \pm 0.2$ dyn cm^{-2}. Although some of the mean bioluminescence data for $\tau_{wall} < 1$ dyn cm^{-2}

were above background, these data were not included for threshold calculations due to the poor correlation between mean bioluminescence and τ_{wall} throughout this range. For laminar flows with τ_{wall} between 1–10 dyn cm^{-2}, spring and summer pooled mean bioluminescence intensity increased as the 2.0 ± 0.3 power of τ_{wall}. For turbulent flow there was a dramatic difference in mean bioluminescence intensity between spring and summer (Fig. 3A). However, there was no significant difference in the mean slope ($t = 0.451$; d.f. = 4; $P = 0.68$). For turbulent flows with τ_{wall} values of 19–950 dyn cm^{-2}, mean bioluminescence intensity for the spring and summer pooled data increased as the 1.1 ± 0.2 power of τ_{wall}.

The corresponding spring maximum bioluminescence data for laminar flow increased about two orders of magnitude between threshold and transition (Fig. 3B). Through transition from laminar to turbulent flow, maximum bioluminescence intensity remained essentially unchanged. Throughout a decade of turbulent flow, $\tau_{wall} = 100 - 1000$ dyn cm^{-2}, maximum bioluminescence continued to remain nearly constant, even as L_{Kwall} became an order of magnitude less than the size of the luminescent dinoflagellates. The relatively small increase in maximum bioluminescence with τ_{wall} to the 0.22 power in turbulent flow was most likely due to the observed increase in flash overlap with increasing flow. Maximum bioluminescence for the 1994 summer data for the 0.85-cm i.d. pipe (not shown) was similar to the spring data, but had greater variability due to the relatively low concentrations of luminescent organisms present.

The bioluminescence potential index during summer 1994 was approximately 10 times less than that measured during the spring (Table 3). A similar decrease in bioluminescence potential was recorded by a bathyphotometer moored approximately 100 m from our collection site. Over a 4 year period, the decrease in bioluminescence potential was seasonal and attributed to a decline in the luminescent dinoflagellates *Protoperidinium* spp. and *L. polyedrum* (Lapota, 1998). This trend was correlated to storm runoff from rainfall in the winter and spring months that enters SD Bay and contains high levels of nutrients. Normalizing
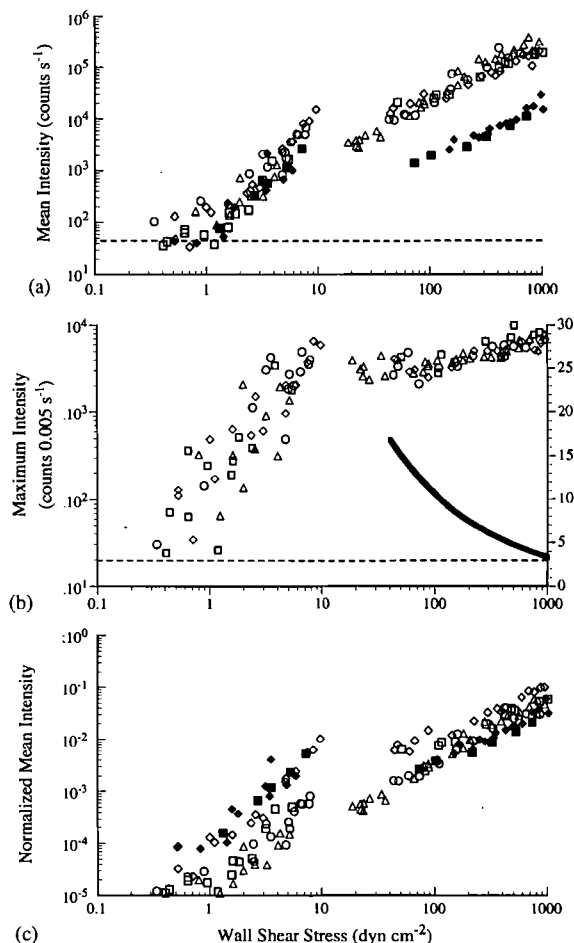

Fig. 3. Luminescent response of mixed plankton samples tested in the 0.85-cm i.d. pipe apparatus. Samples were collected from SD Bay during spring (open symbols) and summer (closed symbols) of 1994. As in Fig. 2. (A) Mean intensity as a function of wall shear stress. (B) Maximum intensity as a function of wall shear stress. (C) Mean intensity normalized by the bioluminescence potential index (Table 3). The gap in the data between τ_{wall} of 10–19 dyn cm^{-2} is the region where transition from laminar to turbulent flow occurred. Symbols designate experimental dates: 4/28/94—open square; 5/01/94—open diamond; 5/09/94—open triangle; 5/10/94—open circle 7/27/94—closed diamond; 8/18/94—closed square.

mean bioluminescence measurements obtained in the 0.85-cm i.d. pipe flow by the corresponding bioluminescence potential index decreased the differences between the spring and summer turbulent flow data (Fig. 3C). Conversely, a similar scaling of mean bioluminescence data collected in

laminar pipe flow increased the disparity between spring and summer data (Fig. 3C).

5. Computational results

Simulations for the turbulent shear stress in the wake of an aircraft carrier moving at $9 \, \mathrm{m \, s^{-1}}$ are presented as contour plots on a plane perpendicular to the ocean surface at the wake centerline (Fig. 4A), and in plan view at the ocean surface (Fig. 4B). Generally, the lowest turbulent stress levels were at the subsurface wake edges. The highest turbulent stresses occurred within the propeller jets and where the turbulence field interacted with the free surface to form regions of strong vorticity on either side of the centerline. These regions were the most persistent wake flow features. The wake volume and corresponding dimensions over which turbulent shear stress levels of 1, 10, 100 and 1000 $\mathrm{dyn \, cm^{-2}}$ were obtained or exceeded were calculated (Table 4).

Choosing a threshold value of 1 $\mathrm{dyn \, cm^{-2}}$ resulted in a potential bioluminescence "footprint" extending throughout the entire simulated wake (Figs. 4A and B). The simulated bioluminescent wake was about 6.6 km in length, 170 m in

width and 18 m in depth, with a total volume of $6.4 \times 10^{6} \, \mathrm{m^{3}}$. For turbulent shear stress thresholds of 10, 100 and 1000 $\mathrm{dyn \, cm^{-2}}$, the bioluminescent wake volume was reduced by 4%, 56% and 95%, respectively (Table 4). The small difference between supra-threshold volumes associated with turbulent shear stress levels greater than 1 and 10 $\mathrm{dyn \, cm^{-2}}$ was due to the large gradients in turbulent shear stress at the wake edge. If laboratory and simulation comparisons were restricted to turbulent shear stresses, the lowest turbulent shear stress attained in the present pipe flow was about 20 $\mathrm{dyn \, cm^{-2}}$ (Fig. 3A, 05/09/94). Assuming a more conservative turbulent shear stress threshold of 100 $\mathrm{dyn \, cm^{-2}}$, the simulations predicted that for suitable viewing conditions and bioluminescence potential, the wake of an aircraft carrier would be observable for 5.4 km.

Several possible relationships between shear stress and energy dissipation rate have been previously noted (Eq. (1), $k = 1, 10/\pi, 7.5$). If it is assumed that a local stress level of at least 1 $\mathrm{dyn \, cm^{-2}}$ is necessary to stimulate bioluminescence then these relationships suggest, to one significant figure, corresponding levels of threshold dissipation for bioluminescence stimulation of 100, 300 and 700 $\mathrm{cm^{2} \, s^{-3}}$. For later comparisons with oceanic dissipation estimates, a broad threshold range between 10^{2}–$10^{3} \, \mathrm{cm^{2} \, s^{-3}}$ is assumed. Dissipation rate estimates within the wake decayed more rapidly than turbulent shear stress (Fig. 5), and, consequently, smaller wake volumes of stimulated bioluminescence are predicted (Table 4). For a threshold value of 100 $\mathrm{cm^{2} \, s^{-3}}$, the maximum length, width and depth of the bioluminescent wake "footprint" was 960, 54 and 6 m, respectively. The associated volume of supra-threshold hydrodynamic stimulus was $1.7 \times 10^{5} \, \mathrm{m^{3}}$. When threshold values of 300 and 700 $\mathrm{cm^{2} \, s^{-3}}$ were used in the simulation the corresponding volumes of supra-threshold dissipation were reduced about 53% and 76%, respectively (Table 4). Because of the high gradients of dissipation occurring at many of the deepest and widest boundaries of the wake, the simulation indicates that there is no difference for maximum depth and width between the dissipation levels chosen.

Table 3
Index of bioluminescence potential measured for the 0.85-cm i.d. pipe flow experiments using mixed plankton collected in San Diego Bay. Values represent means ± standard deviations with number of measurements in parentheses. Bioluminescence potential was higher during the spring than in the summer of 1994

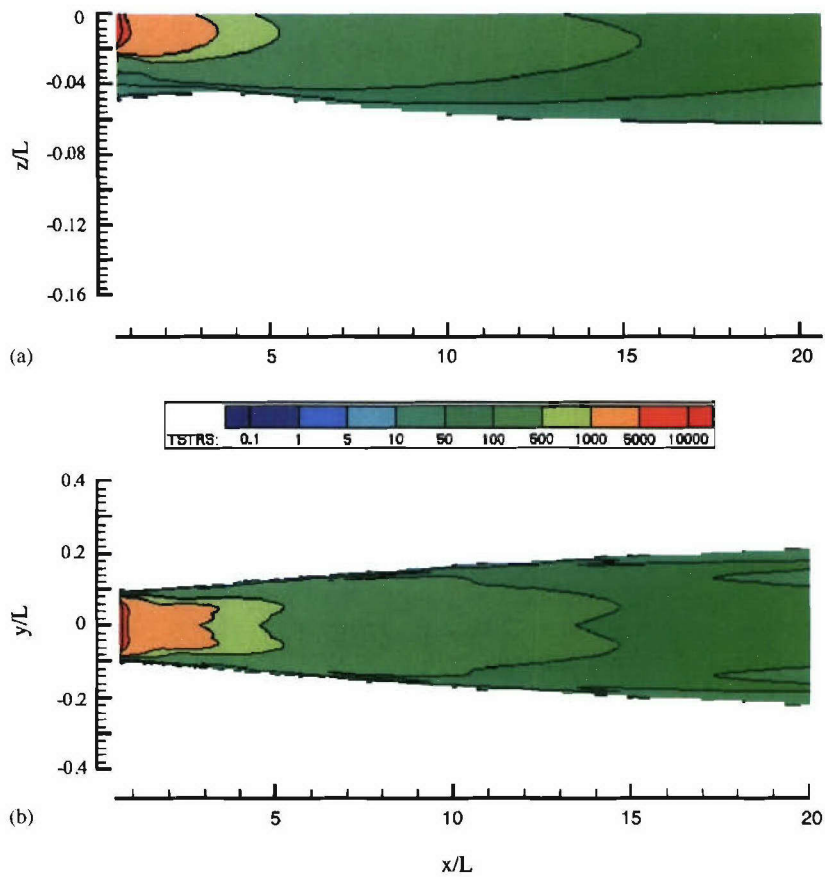| Date	Bioluminescence potential index ($\times 10^{6} \, \mathrm{counts \, s^{-1}}$)	
	Laminar flow	Turbulent flow
Spring 1994		
4/28/94	3.3 ± 1.0 (4)	3.2 ± 0.89 (4)
5/01/94	1.5 ± 0.34 (4)	2.0 ± 1.3 (4)
5/09/94	8.1 ± 0.83 (3)	6.6 ± 1.0 (6)
5/10/94	8.7 ± 1.80 (2)	6.0 ± 1.9 (5)
Summer 1994		
7/27/94	0.52 ± 0.1 (4)	0.47 ± 0.12 (5)
8/18/94	0.49 ± 0.03 (2)	0.51 ± 0.02 (3)

Fig. 4. Turbulent shear stress (units of dyn cm^{-2}) field generated by the numerical simulation of an aircraft carrier moving at 9 m s^{-1}. Depth (z), length (x) and width (y) of the wake are nondimensionalized by the waterline length ($L = 332.5$ m) of the carrier. (A) Axial plane on wake centerline. (B) Plan view at the free surface.

Table 4
Numerical simulation predictions of possible bioluminescent "footprints" for an aircraft carrier moving at 9 ms^{-1}, based on threshold turbulent shear stress stimulation levels of 1, 10, 100 and 1000 dyn cm^{-2}, and threshold dissipation stimulation levels of 100, 300 and 700 cm^2 s^{-3}

Parameter	Wake volume (m^3) where τ is exceeded	Maximum length (m)	Maximum width (m)	Maximum depth (m)
Shear stress, τ (dyn cm^{-2})				
1	6,464,000	6600	172	18
10	6,220,000	6600	170	18
100	2,850,000	5400	166	12
1000	320,000	1100	66	7
Dissipation, ε (cm^2 s^{-3})				
100	169,000	960	54	6
300	80,000	660	54	6
700	40,000	450	54	6

6. Discussion

6.1. Repeatability of pipe flow bioluminescence measurements

For bioluminescence to be a useful method for flow visualization in the ocean, its general response to flow agitation must be fairly repeatable. Where comparisons can be made for both freshly collected mixed plankton samples (Rohr et al., 1990, 1997) and laboratory cultures of the red-tide dinoflagellate *L. polyedrum* (Latz and Rohr, 1999), consistent response patterns are generally found (Table 5). For example, response thresholds always occurred in laminar flow with τ_{wall} on the order of $1 \, dyn \, cm^{-2}$ $(0.1 \, N \, m^{-2})$. Furthermore, for all pipe flow experiments, maximum bio-luminescence measurements were relatively constant for τ_{wall} values greater than about $10 \, dyn \, cm^{-2}$, regardless of whether the flow was laminar or turbulent. The repeatability of the response of luminescent dinoflagellates to flow stimulation is remarkable, given the many factors that can influence bioluminescence. Bioluminescence levels depend not only on species assemblage (Latz et al., 1994; Latz and Lee, 1995) and abundance (Latz and Rohr, 1999), but also on environmental conditions such as light (Sweeney et al., 1959; Sullivan and Swift, 1995; Seliger et al., 1969), temperature (Hastings and Sweeney, 1957; Sweeney, 1981), nutrients (Buskey et al., 1992; Latz and Jeong, 1996), and shear stress history (Latz and Rohr, 1999).
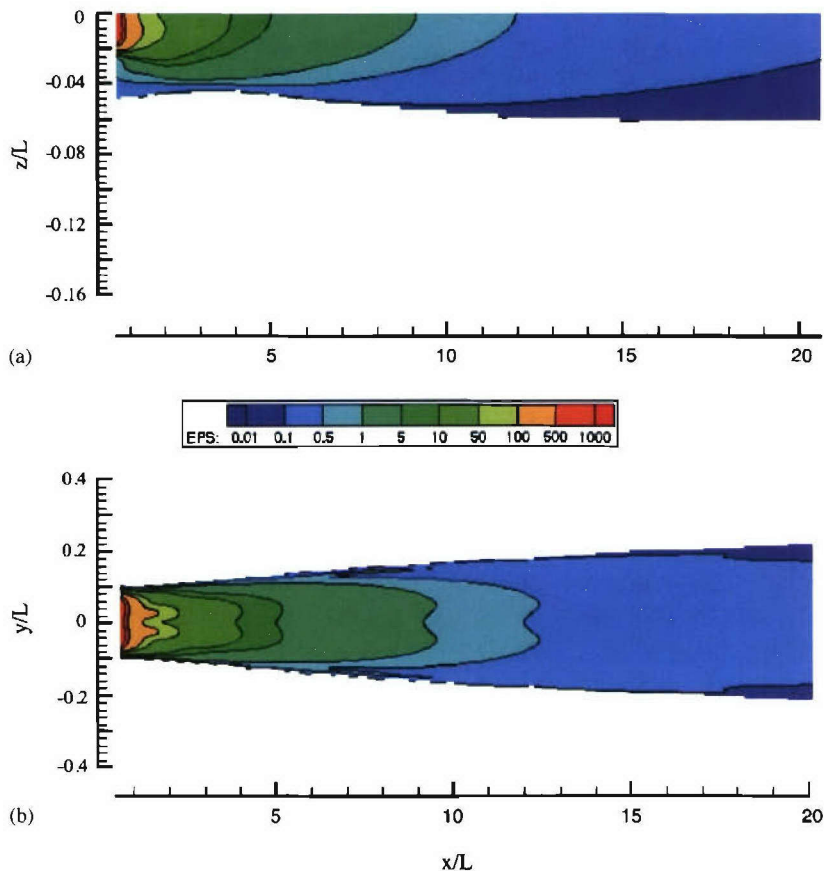

Fig. 5. Energy dissipation per unit mass (units of $cm^2 \, s^{-3}$) field generated by the numerical simulation of an aircraft carrier moving at $9 \, m \, s^{-1}$. As in Fig. 4. (A) Axial plane on wake centerline; (B) Plan view at the free surface.

Table 5
Comparison of pipe flow bioluminescence response trends as a function of wall shear stress, τ_{wall}. Mean slope is calculated from the least-squares regression of log mean bioluminescence intensity vs. τ_{wall}; values represent mean $\pm$ standard deviation with number of experiments in parentheses. Laminar flows occurred for $\tau_{wall} < 20\,dyn\,cm^{-2}$, whereas for $\tau_{wall} > 20\,dyn\,cm^{-2}$ the flow was turbulent

Luminescent source and location	Pipe diameter (cm)	Threshold τ_{wall} ($dyn\,cm^{-2}$)	Mean slope	
			Laminar	Turbulent
Mixed plankton SD Bay and SIO Pier	0.64	1.1 ± 0.3 (12)	1.8 ± 0.3 (12)	
	0.85	0.8 ± 0.2 (6)	2.0 ± 0.3 (6)	1.1 ± 0.2 (6)
Mixed plankton[a] SD Bay	0.64	1 (2)	2.5 (2)	1.0 (4)
Mixed plankton[b] Sea of Cortez	0.64			1.3 (1)
L. polyedrum[c] $<1\,cells\,ml^{-1}$	0.64	4.3 ± 0.5 (5)	2.3 ± 0.5 (4)	
L. polyedrum[c] ≈ 6–$15\,cells\,ml^{-1}$	0.64	3 ± 0.4 (12)	3.7 ± 0.4 (12)	
L. polyedrum[c] $\approx 10^2$–$10^3\,cells\,ml^{-1}$	0.64	2.1 ± 0.03 (3)	5.0 ± 1 (3)	
L. polyedrum[c] $\approx 10^3\,cells\,ml^{-1}$ (Red tide off SIO)	0.64	2.1 (1)		

[a] Rohr et al. (1997).
[b] Rohr et al. (1990).
[c] Latz and Rohr (1999).

Many of the response differences between laboratory cultures of *L. polyedrum* (Latz and Rohr, 1999) and the present mixed plankton experiments may be due to species assemblage. For example, threshold values for the mixed plankton experiments were typically less than those associated with cultures of *L. polyedrum* (Table 5) and maximum bioluminescence levels were greater. These differences could be caused by the presence of the dinoflagellates *C. fusus* and *Protoperidinium* spp. in the mixed plankton experiments. *C. fusus* has a lower response threshold than *L. polyedrum* (Nauen, 1998), and *Protoperidinium* spp. produce brighter flashes (Latz and Jeong, 1996).

Including the *L. polyedrum* experiments, where cell concentrations spanned over four orders of magnitude, threshold τ_{wall} values for cultured and mixed plankton experiments varied between 0.6–$6.0\,dyn\,cm^{-2}$ over 47 laminar, pipe flow experiments (Table 5). Higher average threshold τ_{wall} values of ($4.3 \pm 0.5\,dyn\,cm^{-2}$) were found for *L. polyedrum* concentrations $<1\,cell\,ml^{-1}$ (Latz and Rohr, 1999). Higher threshold values are expected at low cell concentrations because of the low probability of observing bioluminescent flashes at threshold levels for dilute cell concentrations. At high concentrations (10^2–$10^4\,cells\,ml^{-1}$) of *L. polyedrum*, threshold τ_{wall} values are between

1–$2\,dyn\,cm^{-2}$ for both pipe (Latz and Rohr, 1999) and Couette (Latz et al., 1994) flow.

Cell concentration also affects the slope of the power regression of mean bioluminescence as a function of τ_{wall} (Latz and Rohr, 1999). In laminar flow, increasing concentrations of cultured *Lingulodinium polyedrum* (<1–$10^3\,cell\,ml^{-1}$) result in higher values of the mean slope (2.3–5.0) of log mean bioluminescence vs. log τ_{wall} (Table 5). The slope increases, because at high laminar flows mean bioluminescence scales with cell concentration, whereas background levels, which do not scale with cell concentration, dominate mean bioluminescence near the response threshold. In turbulent flow, the rate of increase of mean bioluminescence with τ_{wall} is insensitive to the background levels of the detector. Consequently, the power law dependence of mean bioluminescence on τ_{wall} should be independent of cell concentration in turbulent flow. For the 11 mixed plankton experiments where data are available for turbulent flow the power-law dependence of mean bioluminescence on τ_{wall} ranged from 0.9 to 1.3 (Table 5).

For all experiments the power law dependence of mean bioluminescence on τ_{wall} varied conspicuously between laminar and turbulent flow. For the present mixed plankton studies, a representative power law for laminar flow was about 2 (1.9 ± 0.3,

$n = 18$) and for turbulent flow about 1 (1.1 ± 0.2, $n = 6$). This dramatic change in slope can be attributed to several factors. The maximum flash response of individual cells increases dramatically with τ_{wall} from threshold to about $10\,dyn\,cm^{-2}$, but at higher laminar and throughout turbulent flow, maximum bioluminescence measurements remain essentially constant (Rohr et al., 1997; Latz and Rohr, 1999; present data). The proportion of responding cells is also thought to increase with τ_{wall} at a much higher rate in laminar than turbulent flow (Latz and Rohr, 1999). Finally, τ_{wall} increases to the first power of U_{avg} in laminar flow, but to the 1.75 power of U_{avg} in turbulent flow (Schlichting, 1979). Therefore, U_{avg} and related advection effects increase more slowly in turbulent than laminar flow for equal increments of τ_{wall}. For example, if mean bioluminescence measurements when expressed as counts per second increase as the 2nd power of τ_{wall} in laminar flow and the 1st power of τ_{wall} in turbulent flow, then when expressed as counts per volume the powers are disproportionately decreased to 1 and 0.43.

The difference in bioluminescence potential indices between the spring and summer of 1994 were reflected by nearly equal differences in the corresponding mean bioluminescence intensities for the 0.85-cm i.d. turbulent pipe flows. These results suggest that the present bioluminescence potential index is proportional to the biomass of luminescent organisms stimulated in turbulent flow. Rohr et al. (1990) also noted a lack of correlation between bioluminescence potential, using an identical shipboard flow agitator, and laminar pipe flow, using a similar 0.635-cm i.d. pipe apparatus. In laminar flow the correlation coefficient was 0.3, whereas in turbulent flow it was 0.8. The poor correlation between bioluminescence potential and the bioluminescence of mixed plankton measured in high laminar pipe flow is not observed for cultures of L. polyedrum, where both high laminar pipe flow measurements and bioluminescence potential scale with cell concentration (unpublished data). Unlike L. polyedrum, some of the luminescent organisms present in the mixed plankton samples may be stimulated by the turbulence of the flow agitator but not in the range of laminar pipe flows provided.

6.2. Caveats for laboratory/ocean comparisons

The hydrodynamic response thresholds for luminescent dinoflagellates determined exclusively in laminar laboratory flows were applied to ship wakes and oceanic flows that are unmistakably turbulent. There are several precedents for applying measurements obtained in laboratory laminar flows directly to turbulent, oceanic processes (Lazier and Mann, 1989; Thomas and Gibson, 1990a, b, 1992; Mead and Denny, 1995). The common argument is that organisms less than the smallest energetic eddy scales reside is a laminar, approximately linear, velocity gradient whose magnitude is determined by the dissipation (Lazier and Mann, 1989; Estrada and Berdalet, 1997). Thus at the small spatial scales of the organisms, oceanic turbulence is experienced as a laminar shear.

Different turbulent length scales have been used as a measure of the smallest energetic eddy within which smaller entrained organisms should experience laminar flow. Thomas and Gibson (1990a, 1992) used the convenient value of L_K, noting that in the ocean L_K is seldom less than 1 mm, and that the dinoflagellates in their study (which included L. polyedrum), are less than an order of magnitude smaller. Mann and Lazier (1996) consider the smallest turbulent eddies in a highly energetic environment to be about 6 mm. Because L_K is derived from dimensional analysis, it can only serve as an estimate for the smallest length scales of the turbulence. Measurements of turbulent scales within the surface mixed layer of the ocean (Oakey and Elliot, 1980) indicate that maximum shear energy occurs at about $40L_K$ (Lazier and Mann, 1989). Mead and Denny (1995) use $40L_K$ as their cutoff and submit that a sea urchin egg of 80–110 μm in diameter will experience laminar flow in the surf zone or benthic boundary layer when $40L_K$ is as small as 200–880 μm. Experimental spectra for different flows suggest that the actual limit of the dissipation range is closer to $10L_K$ (Jimenez, 1997; Catalan, 1999). For the present study, $10L_K$ was chosen as representative of the smallest energetic turbulent length scales within which laminar flow presides. By this criterion, if $10L_K$ is larger than about 500 μm, then all the

dinoflagellates of interest should experience essentially laminar flow. A threshold τ_{wall} value of $1\,\mathrm{dyn\,cm}^{-2}$ and $k = 1$ results in $\varepsilon = 91\,\mathrm{cm}^2\,\mathrm{s}^{-3}$ and $10\,L_K = 1063\,\mu\mathrm{m}$. For $k = 7.5$, $10L_K = 642\,\mu\mathrm{m}$. Regardless of the exact value of k and threshold τ_{wall}, the organisms were smaller than $10L_K$ and therefore should experience the turbulence as a laminar flow.

At small scales intermittency is a general feature of turbulent flows (Gregg et al., 1993; Estrada and Berdalet, 1997), and fluctuating shear has been thought to increase cell sensitivity (Anderson et al., 1988). Nevertheless, an implicit assumption shared by all these studies is that the response of organisms to flow parameters studied in *steady* laminar flow will be similar in the *unsteady* laminar flow of the smallest turbulent eddies within which they reside. The pipe flow data provide some evidence that the fluctuating nature of turbulence, even at length and time scales relevant to the organisms, is not always exceptionally stimulatory. For example, for the 0.64-cm i.d. pipe experiments, while levels of τ_{wall} and ε increased about 4- and 20-fold, respectively, through transition from laminar to turbulent flow, mean bioluminescence increased much less, approximately doubling, and maximum bioluminescence remained nearly constant. The lowest wall shear stress values obtained in turbulent pipe flow are about $20\,\mathrm{dyn\,cm}^{-2}$, and have been reported as no more stimulatory as the same shear stress in laminar pipe flow (Latz and Rohr, 1999). The insensitivity of maximum bioluminescence levels to the length and time scales of the turbulence is particularly notable given the significant shear sensitivity reported for plant and animal cells (reviewed by Hua et al., 1993).

Numerical simulations and oceanic measurements provide descriptions of the flow field that are averaged over length and time scales much larger than what are directly relevant to the organisms of interest. To borrow the terminology of Catalan (1999), whereas the pipe flow studies can provide detailed information of the "hydrodynamic weather" that individual plankton are experiencing, the numerical simulations and oceanographic measurements can only provide an indicator of their "hydrodynamic climate". Nevertheless, climate and weather are related, and

laboratory experiments provide the beginnings of a scientific context to interpret observations of flow-induced bioluminescence in the ocean. For the purpose of this initial comparison, oceanic flow fields providing average shear stress levels exceeding those determined in laminar pipe flow as threshold levels (greater than $1\,\mathrm{dyn\,cm}^{-2}$ which is equivalent to dissipation rates $\sim 10^2$–$10^3\,\mathrm{cm}^2\,\mathrm{s}^{-3}$) are considered as viable candidates for flow visualization in the ocean.

6.3. Ship wake bioluminescence observations

A frequently observed bioluminescent flow field is the nighttime wake of a ship. Ship wake bioluminescence is sufficiently ubiquitous to map the spatial distributions of luminescent organisms at the sea surface (Bityukov, 1971). Aviators have relied on the bioluminescent wake of an aircraft carrier to help relocate their ship at night (Hastings, 1993; Lovell and Kluger, 1994). Zeppelins and planes have similarly used bioluminescent wakes to search for enemy surface ships (Tarasov, 1956), and surface ships have used bioluminescent wakes to detect and track submarines (Staples, 1966).

The size of the luminescent "footprint" of the wake of an aircraft carrier, predicted by the numerical simulation, was dependent on whether shear stress or energy dissipation thresholds were used. A threshold shear stress of 1–$10\,\mathrm{dyn\,cm}^{-2}$ resulted in a predicted bioluminescent wake length $> 6\,\mathrm{km}$, whereas for a threshold dissipation rate of $100\,\mathrm{cm}^2\,\mathrm{s}^{-3}$, the predicted length was approximately $1\,\mathrm{km}$. This large difference is not surprising given the different assumptions involved in estimating shear stress and dissipation in the simulations. Unfortunately, there are presently no scientific studies and only a few anecdotal references that provide quantitative descriptions of the dimensions of stimulated bioluminescence within a ship's wake. Moreover, observations of ship wake bioluminescence depend on many contributing factors, including the bioluminescence potential of the seawater, the distribution and magnitude of supra-threshold agitation levels within the wake, background ambient light, the state of dark adaptation of the observer's eyes, and the height

of the observer above the sea surface. The presence of bubbles throughout the wake can also affect one's perception of the bioluminescence within it (Tarasov, 1956; Vasil'kov et al., 1992).

Tarasov (1956) and Turner (1965) recount tales of bioluminescent ship wakes estimated to be of the order of a mile (1.6 km) long. The distance to the horizon, correcting for refraction effects (French, 1982), for an observer whose eyes are 2–10 m above sea level are greater than this distance, ranging from about 3.4–7.7 miles (5.5–12.4 km). However, viewing bioluminescence wakes from the ship creating them is generally a poor vantage point because the percentage of competing skylight reflected from the ocean surface increases dramatically towards the horizon (Lynch and Livingston, 1995). Aerial observations provide a much better view. Anecdotal accounts of World War II carrier-based aviators describe luminescent wakes that could sometimes be seen for miles (Hastings, 1993). Observations of wake-stimulated bioluminescence extending several miles (about 10 or more aircraft carrier boat lengths) are consistent with the numerical simulation estimates for a threshold turbulent shear stress of $1–10 \, \mathrm{dyn \, cm^{-2}}$. Most of our observations from the stern of smaller ships (Rohr, personal observations) are more in accord with estimates of 1–2 boat lengths, which would be better predicted by the simulation estimates using threshold dissipation values of about $100 \, \mathrm{cm^2 \, s^{-3}}$. Observations of ship wake bioluminescence during which the appropriate optical and biological ground truth measurements are collected could provide effective transfer functions between simulations, laboratory studies, and field predictions and ultimately provide opportunities to validate the simulations as well.

6.4. Oceanic flows and shear stress thresholds for bioluminescence stimulation

Spectacular bioluminescence displays have been associated with the movement of dolphins (Rohr et al., 1998), torpedoes (Shaw, 1959), fish (Harvey, 1952), and divers (Lythgoe, 1972; Robinson, 1998). The bioluminescent "signatures" of some swimming fish are distinct enough that they have

been used to differentiate species (Roithmayr, 1970; Morin, 1983). Along moving boundaries the pipe flow results are directly applicable. Applying the Blasius flat-plate boundary layer solution, a laminar flow of $26 \, \mathrm{cm \, s^{-1}}$ ($\approx 0.5 \, \mathrm{knot}$) over a 20-cm long flat plate will produce shear stresses $> 1 \, \mathrm{dyn \, cm^{-2}}$ everywhere on the plate (Schlichting, 1979). Conspicuous bioluminescence features on a moving body will occur where the volume of supra-threshold flow changes abruptly, e.g., where separation or boundary layer transition occurs. Many of these bioluminescence features have been observed in studies of flow-stimulated bioluminescence associated with swimming dolphins (Rohr et al., 1998). It is attractive to look for geophysical phenomena where bioluminescence could be used as an indicator of highly energetic flows.

The oceanic implications of a threshold shear stress of the order of $1 \, \mathrm{dyn \, cm^{-2}}$ are noteworthy. More than 70 years ago, Harvey (1929) posed the question of what use flow-stimulated bioluminescence could be for a protozoan, living at the surface of the sea, "blown hither and thither by the wind." For dinoflagellate bioluminescence to be an effective anti-predator strategy (Burkenroad, 1943; Esaias and Curl, 1972; Buskey et al., 1983; Morin, 1983; Abrahams and Townsend, 1993) organisms should not continually be stimulated by oceanic ambient motion. A threshold shear stress level of $1 \, \mathrm{dyn \, cm^{-2}}$ is consistent with this assumption. In the ocean interior, where background dinoflagellate bioluminescence is rare (Boden et al., 1965; Widder et al., 1989; Buskey and Swift, 1990), a shear stress level of $1 \, \mathrm{dyn \, cm^{-2}}$ is typically several orders of magnitude higher than ambient levels associated with oceanic turbulence (Oakey and Elliott, 1982; Evans, 1982; Yamazaki and Osborn, 1988; Haury et al., 1990; Thomas and Gibson, 1990a; Mann and Lazier, 1996).

Naturally occurring flow fields associated with threshold shear stress levels greater than or equal to $1 \, \mathrm{dyn \, cm^{-2}}$ are most likely to occur at the ocean's boundaries. Estimates of fluid drag on the ocean floor due to topographic waves are typically of the order of $0.5 \, \mathrm{dyn \, cm^{-2}}$ (Bell, 1978). Tidal currents (Bowden et al., 1959; Sternberg, 1968; Cheng et al., 1999), high-energy deep-sea currents

(Gross and Nowell, 1990), hurricanes (Gardner et al., 2001), and the surf zone (Cox et al., 1996) have been estimated to produce bottom shear stresses of the order of 1 to $10\,\mathrm{dyn\,cm^{-2}}$. Wave-forced bottom shears in shallow near-shore areas have also been reported in this same range (Sanford, 1993). A value of about $1\,\mathrm{dyn\,cm^{-2}}$ is the critical erosion stress for 0.1-mm diameter quartz grains in water (Inman, 1949; Miller et al., 1977) and for many cohesive types of sediment as well (Mehta et al., 1982). Another flow candidate for bioluminescence stimulation at the ocean bottom is internal solitary waves. Observations of resuspension under the footprint of internal wave packets reveal a marked increase in particulates up to 10 m above the ocean bottom (Bogucki and Redekopp, 1999). Supra-threshold shear levels can be also found within the ocean surface shear stress layer, but only over very shallow depths. A typical wind speed of $7\text{--}8\,\mathrm{m\,s^{-1}}$ at mid-latitudes will produce a surface stress layer of $1\,\mathrm{dyn\,cm^{-2}}$ (Gill, 1982; Pond and Pickard, 1983) over a depth of about 2 mm (Phillips, 1980).

Rainfall has been considered as another candidate source for naturally occurring bioluminescence at the ocean surface (Tarasov, 1956). The vertical stresses produced in the water at the sea surface due to both light ($0.4\,\mathrm{cm\,h^{-1}}$) and moderate ($4.3\,\mathrm{cm\,h^{-1}}$) falling rain have been calculated to be $<1\,\mathrm{dyn\,cm^{-2}}$ (Manton, 1973). Even with a wind speed of $10\,\mathrm{m\,s^{-1}}$, surface shear stresses produced by a rainfall rate of $2.5\,\mathrm{cm\,h^{-1}}$ are estimated to be less than threshold (Caldwell and Elliott, 1971). Therefore, rainfall is not predicted to stimulate bioluminescence based on the shear stresses generated. Furthermore, based on the kinetic energy flux at the surface (Ho et al., 1997) for heavy rain dissipated over a depth of 10 cm (Manton, 1973) estimated dissipation rates are several orders of magnitude less than threshold values of $10^2\text{--}10^3\,\mathrm{cm^2\,s^{-3}}$.

However, rain drops 0.8–1.1 mm in diameter, which are common in light rain, create bubbles of approximately $440\,\mu\mathrm{m}$ diameter when they fall at normal incidence to a plane water surface (Pumphrey et al., 1989; Medwin and Clay, 1998). Even significantly smaller bubbles, of the order of $100\text{-}\mu\mathrm{m}$ diameter, can provide supra-threshold

levels of flow stimulation as they rise (Bavarian et al., 1991). Bubbles within this diameter range and larger have been found near breaking waves (Medwin and Daniel, 1990; Leighton, 1997) and in ship wakes (Hyman, 1994) and may be an important component of their bioluminescent signatures. Laboratory studies, albeit with much larger bubble diameters of 0.1–1.8 cm, have found rising bubbles to stimulate the bioluminescence of *Linguidinium polyedrum* (Anderson et al., 1988; Latz and Case, unpublished observations).

Although there have been anecdotal accounts of bioluminescence highlighting water current structure in the ocean surface layer (Tarasov, 1956), there are no known scientific studies directed towards observing naturally occurring, flow-stimulated bioluminescence at the ocean's boundaries. The lack of observations may in part be due to the avoidance by luminescent organisms of flow regions of high agitation (Tynan, 1993) and a paucity of nighttime in situ observations under favorable conditions.

6.5. Pressure vs. shear stress thresholds for bioluminescence stimulation

Dinoflagellate bioluminescence is relatively insensitive to pressure. For example, a static pressure of $1\,\mathrm{dyn\,cm^{-2}}$, the shear stress response threshold, corresponds to a height of seawater of about 0.01 mm, so that supra-threshold levels would exist essentially throughout the entire ocean. Laboratory studies with cultures of *L. polyedrum* show that only at extremely high pressures, of the order of $10^7\,\mathrm{dyn\,cm^{-2}}$ (25 atm), does static pressure affect the rate of spontaneous flashing (Gooch and Vidaver, 1980; Swift et al., 1981). Considering the effect of varying pressure, which has been proposed to provide greater stimulation (Anderson et al., 1988), a plane wave in seawater with a rms of $1\,\mathrm{dyn\,cm^{-2}}$ has an associated sound intensity of $6.4 \times 10^{-9}\,\mathrm{W\,m^{-2}}$. This intensity is lower than the mean level of ambient sea noise (Tavolga, 1967), again suggesting that throughout the ocean there would be continuous bioluminescence stimulation. In regards to bioluminescent ship wakes, the radiated noise at 1 m from a large ship can be 10^4 times greater than $1\,\mathrm{dyn\,cm^{-2}}$

(Richardson et al., 1995). Assuming spherical spreading, only at distances > 10 km in any direction from the ship would pressure amplitudes in the water drop below 1 dyn cm^{-2}. Based on the absence of these bioluminescence observations, stimulatory oscillating pressure amplitudes must be significantly > 1 dyn cm^{-2}. Indeed, for cultures of *L. polyedrum*, much larger pressure amplitude variations, on the order of 10^6 dyn cm^{-2} s^{-1}, are necessary for bioluminescence stimulation (Krasnow et al., 1981; Donaldson et al., 1983).

6.6. Oceanic flows and dissipation thresholds for bioluminescence stimulation

Energetic hydrodynamic events occurring within the ocean are often characterized by dissipation estimates based on the smallest scales of the velocity or temperature gradient. However, these measurements are often difficult to obtain (Anis and Moum, 1995; Veron and Melville, 1999) and order of magnitude values of dissipation are often considered questionable (Drennan et al., 1996). Furthermore, oceanic dissipation rates exhibit significant spatial and temporal variations (Oakey and Elliott, 1982; Yamazaki and Lueck, 1990; Agrawal et al., 1992; Gregg et al., 1993). Consequently the possibility of obtaining a near instantaneous, synoptic view of highly dissipative events through flow-induced bioluminescence would be most appealing.

There are many studies providing average dissipation values for various oceanic flows, which when juxtaposed with the pipe flow dissipation thresholds, provide a convenient starting point for initial comparisons. A calculated threshold dissipation rate on the order of 10^2–10^3 cm^2 s^{-3} (10^{-2}–10^{-1} m^2 s^{-3}) for flow-stimulated bioluminescence is many orders of magnitude higher than what has been generally reported within the ocean interior (Osborn, 1980; Crawford and Osborn, 1980; Lueck et al., 1983; Larson and Gregg, 1983; Gargett and Halloway, 1984; Lueck and Osborn, 1986; Sandstrom and Oakey, 1995; Gregg and Ozsoy, 1999; Seim et al., 1999). For example, in the deep ocean ε has been found to be of the order of 10^{-6} cm^2 s^{-3} (Kunze and Sanford, 1996) and of the order of 10^{-1} cm^2 s^{-3} for the upper parts of the oceanic mixed layer (Shay and Gregg, 1984; Gargett, 1989). Maximum values of ε associated with coastal zones (Kiørboe and Saiz, 1995), tidally mixed regions (Grant et al., 1962; Rothschild and Osborn, 1988), internal hydraulic jumps (Farmer and Armi, 1988), breaking internal waves (Lien and Gregg, 2001), and the ocean surface (Soloviev et al., 1988; Anis and Moum, 1995; Drennan et al., 1996; Kitaigorodskii, 1997) are typically between 1 and 10 cm^2 s^{-3}. Seim and Gregg (1997) have reported dissipation levels as large as 10–10^3 cm^2 s^{-3} in tidally forced flow over a sill.

Equally large values of ε have been measured beneath small breaking waves (George et al., 1994; Terray et al., 1996). At the ocean surface, breaking waves are a common source of bioluminescence stimulation (Staples, 1966; Latz et al., 1994). Supra-threshold levels of dissipation associated with small breaking waves is consistent with laboratory observations where 10-cm peak to trough breaking waves stimulated bioluminescence (unpublished data).

Gross estimates of average dissipation levels in the benthic boundary layer, surge channel, and surf zone suggest levels much higher than threshold. Mean dissipation levels in the near-shore, benthic boundary layer, which is expected to be only a few centimeters thick, have been predicted to be as high as 8×10^4 cm^2 s^{-3} (Mead and Denny, 1995). This estimation was based on Eq (1) with $k = 1$, and τ equal to the product of the water density and the friction velocity squared. The friction velocity was assumed to be 5% of the mainstream velocity near the substratum, which in turn was estimated from linear wave theory. Mean dissipation levels within a surge channel have also been estimated to be of the order of 10^4 cm^2 s^{-3} (Denny et al., 1992), calculated by dividing the estimated net wave energy transported across the mouth of the channel by the effective mass of water in which the wave energy is dissipated. Depending on shore slope and wave height, mean energy dissipation rates throughout the surf zone have been predicted to range from about 10^2–10^4 cm^2 s^{-3} on wave-swept rocky shores (Mead and Denny, 1995). Measurements in the laboratory and surf zone by Veron and Melville (1999),

however, show that the turbulence is likely to be dissipated rapidly and locally under individual breakers. Nighttime observations have shown bioluminescence associated with breaking waves, but not between sets of breaking waves (unpublished data). It is not known whether this discrepancy is due to depletion of luminescence of the most shear-sensitive luminescent organisms, incorrect dissipation estimates, or bioluminescence displays too dim to accurately observe. As is the case with ship wakes, such flow fields invite further study.

Some observations of rare bioluminescent events recorded by merchant ships have been attributed to the passage of solitons (Wyatt, 1987). Although average dissipation levels can increase 3 orders of magnitude because of internal solibores (Gregg et al., 1999), these values are still two orders of magnitude below threshold levels for bioluminescence. Nevertheless, the individual energetic events responsible for this large change in the average dissipation may also be another good candidate for bioluminescence flow visualization.

7. Conclusions

The present mixed plankton, pipe flow data obtained over a year at two different locations and in two different pipe flow apparatus clearly exhibited a characteristic luminescent response to repeated flow stimuli. Threshold levels of stimulation always occurred in laminar flow at τ_{wall} values on the order of $1\,\mathrm{dyn\,cm^{-2}}$, with corresponding threshold dissipation values between 10^2 and $10^3\,\mathrm{cm^3\,s^{-2}}$. Differences in mean bioluminescence levels due to changing species abundance were effectively scaled in turbulent flow by dividing mean bioluminescence by the corresponding bioluminescence potential index. Maximum bioluminescence, indicative of individual flash intensities, remained nearly constant throughout both high laminar and all turbulent flow, irrespective of the changing length and time scales of the turbulence. Present data trends are generally in good agreement with previous pipe flow measurements.

Bioluminescence threshold levels were consistent with observations of flow-stimulated bioluminescence associated with boundary layer flows as well as the general lack of observations within internal oceanic flow fields. Because background agitation levels in the ocean interior are generally several orders of magnitude below threshold, flow-induced bioluminescence could be used as an indicator of highly energetic oceanic events. For the present study it was assumed that marine plankton respond similarly to changing and steady laminar flow. This assumption must be verified in light of previous observations (Anderson et al., 1988) suggesting that the rate of change of flow is important. The present study also did not determine threshold levels for turbulent shear stress. Turbulent shear stresses in a bottom mixed layer can be an order of magnitude greater than the threshold laminar shear stress (Stacey et al., 1999a). Relating laboratory measurements, which describe the local hydrodynamic "weather" to which plankton respond, to the climatological indicators afforded by present oceanic measurements and numerical simulations will remain a challenge for some time. Nevertheless, luminescent dinoflagellates inhabit all the world's oceans and could, under proper viewing conditions and for suitable concentrations, act as a robust indicator for highly energetic events in the ocean.

Acknowledgements

References

Abrahams, M.V., Townsend, L.D., 1993. Bioluminescence in dinoflagellates: a test of the burglar alarm hypothesis. Ecology 74, 258–260.

Agrawal, Y.C., Terray, E.A., Donelan, M.A., Hwang, P.A., Williams, A.J., Drennan, W.M., Kahma, K.K., Kitaigorodskii, S.A., 1992. Enhanced dissipation of kinetic energy beneath surface waves. Nature 359, 219–220.

Anderson, D.M., Nosenchuck, D.M., Reynolds, G.T., Walton, A.J., 1988. Mechanical stimulation of bioluminescence in the dinoflagellate Gonyaulaz polyedra Stein. Journal of Experimental Marine Biology and Ecology 122, 277–288.

Anis, A., Moum, J.N., 1995. Surface wave–turbulence interactions: scaling $\varepsilon(z)$ near the sea surface. Journal of Physical Oceanography 23, 2025–2045.

Bakhmeteff, B., 1936. The Mechanics of Turbulent Flow. Princeton University Press, Princeton, NJ, 101pp.

Bavarian, F., Fan, L.S., Chalmers, J.J., 1991. Microscopic visualization of insect–bubble interactions. I. Rising bubbles, air–medium interface, and the foam layer. Biotechnology Program 7, 140.

Bell, T.H., 1978. Radiation damping of inertial oscillations in the upper ocean. Journal of Fluid Mechanics 88, 289–308.

Biggley, W.H., Swift, E., Buchanan, R.J., Seliger, H.H., 1969. Stimulable and spontaneous bioluminescence in the marine dinoflagellates, *Pyrodinium bahamense*, *Gonyaulax polyedra*, and *Pyrocystis lunula*. Journal of General Physiology 54, 96–122.

Bityukov, E.P., 1971. Bioluminescence in the wake of a ship in the Atlantic Ocean and the Mediterranean Sea and Black Sea. Okeanologiya 11, 127–133.

Boden, B.P., Kampa, E.M., Snodgrass, J.M., 1965. Measurements of spontaneous bioluminescence in the sea. Nature 208, 1078–1080.

Bogucki, D.J., Redekopp, L.G., 1999. A mechanism for sediment resuspension by internal solitary waves. Geophysical Research Letters 28 (9), 1317–1320.

Bowden, K.F., Fairbairn, L.A., Hughes, P., 1959. The distribution of shearing stresses in a tidal current. Geophysical Journal 2, 288–305.

Burkenroad, M.D., 1943. A possible function of bioluminescence. Journal of Marine Research 5, 161–164.

Buskey, E.J., Swift, E., 1990. An encounter model to predict natural planktonic bioluminescence. Limnology and Oceanography 35, 1469–1485.

Buskey, E.J., Mills, L., Swift, E., 1983. The effects of dinoflagellate bioluminescence on the swimming behavior of a marine copepod. Limnology and Oceanography 28, 575–579.

Buskey, E.J., Strom, S., Coulter, C., 1992. Bioluminescence of heterotrophic dinoflagellates from Texas coastal waters. Journal of Experimental Marine Biology and Ecology 159, 37–49.

Caldwell, D.R., Elliott, W.P., 1971. Surface stresses produced by rainfall. Journal of Physical Oceanography 1, 145–148.

Catalan, J., 1999. Small-scale hydrodynamics as a framework for plankton evolution. Japan Journal of Limnology 60, 469–494.

Cheng, R.T., Ling, C.H., Gartner, J.W., 1999. Estimates of bottom roughness length and bottom shear stress in South San Francisco Bay, California. Journal of Geophysical Research 104 (C4), 7715–7728.

Clark, G.L., Denton, E.J., 1962. Light and animal life. In: Hill, M.N. (Ed.), The Sea, Vol. 1 (Physical Oceanography). Interscience, New York, pp. 456–468.

Cox, D.T., Kobayashi, K.N., Okayasu, A., 1996. Bottom shear stress in the surf zone. Journal of Geophysical Research 101 (C6), 14337–14348.

Crawford, W.R., Osborn, T.R., 1980. Microstructure measurements in the Atlantic equatorial undercurrent during GATE. Deep-Sea Research 26 (Suppl. II), 285–308.

Davies, J.T., 1972. Turbulence Phenomenon. Academic Press, New York, 412pp.

Denny, M.J., Dairiki, J., Distefano, S., 1992. Biological consequences of topography on wave-swept rocky shores: I. Enhancement of external fertilization. Biological Bulletin 183, 220–232.

Donaldson, T.Q., Tucker, S.P., Lynch, R.V., 1983. Stimulation of bioluminescence in dinoflagellates by controlled pressure changes. Naval Research Laboratory Report 8772, Washington, District of Columbia, 5pp.

Drennan, W.M., Donelan, M.A., Terray, E.B., Katsaros, K.B., 1996. Oceanic turbulence dissipation measurements in SWADE. Journal of Physical Oceanography 26, 808–815.

Eckert, R., 1965. Bioelectric control of bioluminescence in the dinoflagellate *Noctiluca*. Science 147, 1140–1145.

Esaias, W.E., Curl Jr., H.C., 1972. Effect of dinoflagellate bioluminescence on copepod ingestion rates. Limnology and Oceanography 17, 901–906.

Esaias, W.E., Curl, H.C., Seliger, H.H., 1973. Action spectrum for a low intensity, rapid photoinhibition of mechanically stimulable bioluminescence in marine dinoflagellate *Gonyaulax catenella, G. acatenella* and *G. tamarensis*. Journal of Cellular Physiology 82, 363–372.

Estrada, M., Berdalet, E., 1997. Phytoplankton in a turbulent world. Scienta Marina 61 (Suppl. 1), 125–140.

Evans, D.L., 1982. Observations of small-scale shear and density structure in the ocean. Deep-Sea Research 29, 581–595.

Farmer, D.M., Armi, L., 1988. The flow of Atlantic water through the Straight of Gibralter. Progress in Oceanography 21, 1–105.

Fleisher, K.J., Case, J.F., 1995. Cephalopod predation facilitated by dinoflagellate luminescence. Biological Bulletin 189, 263–271.

French, A.P., 1982. How far away is the horizon? American Journal of Physics 50, 795–799.

Gardner, W.D., Blakey, J.C., Walsh, I.D., Richardson, M.J., Pegau, S., Zaneveld, J.R.V., Roesler, C., Gregg, M.C., MacKinnon, J.A., Sosik, H.M., Williams III, A.J., 2001. Optics, particles, stratification, and storms on the New England continental shelf. Journal of Geophysical Research 106 (C5), 9473–9497.

Gargett, A.E., 1989. Ocean turbulence. Annual Review of Fluid Mechanics 21, 419–451.

Gargett, A.E., Halloway, G., 1984. Dissipation and diffusion by internal wave breaking. Journal of Marine Research 42, 15–27.

George, R., Flick, R.E., Guza, R.T., 1994. Observations of turbulence in the surf zone. Journal of Geophysical Research 99 (C1), 801–810.

Gill, A., 1982. Atmosphere-Ocean Dynamics. Academic Press, New York, 662pp.

Gooch, V., Vidaver, W., 1980. Kinetic analysis of the influence of hydrostatic pressure on bioluminescence of *Gonyaulax polyedra*. Photochemical Photobiology 31, 397–402.

Grant, H.L., Stewart, R.W., Moilliet, A., 1962. Turbulence spectra from a tidal channel. Journal of Fluid Mechanics 12, 241–268.

Gregg, M.C., Ozsoy, E., 1999. Mixing on the Black Sea Shelf North of the Bosphoros. Geophysical Research Letters 26, 1869–1872.

Gregg, M.C., Seim, H.E., Percoval, D.B., 1993. Statistics of shear and turbulent dissipation profiles in random internal wave fields. Journal of Physical Oceanography 23, 1777–1799.

Gregg, M.C., Winkel, D.W., MacKinnon, J.A., Lien, R.C., 1999. Mixing over shelves and slopes. In: Muller, P., Henderson, D. (Eds.), Dynamics of Oceanic Internal Gravity Waves, II, Proceedings of the Hawaiian Winter Workshop. University of Hawaii, Honolulu, pp. 35–42.

Gross, T.F., Nowell, A.R.M., 1990. Turbulent suspensions of sediments in the deep sea. Philosophical Transactions of the Royal Society of London, Series A 331, 167–181.

Harvey, E.N., 1929. Phosphorescence. Encyclopedia Brittanica, 14th Edition, Vol. 17, University of Chicago, Chicago, IL, p.780.

Harvey, E.N., 1952. Bioluminescence. Academic Press, New York, 646pp.

Harvey, E.N., 1957. A History of Bioluminescence. American Phil. Society Philadelphia, Baltimore, MD.

Hastings, J.W., 1993. Dinoflagellates: cell biochemistry and its regulation of the millisecond and 24 hour time scale. Naval Research Reviews XLV, 21–30.

Hastings, J.W., Sweeney, B.M., 1957. On the mechanism of temperature independence in a biological clock. Proceedings of the National Academy of Science USA 43, 804–811.

Haury, L.R., Yamazaki, H., Itsweire, E.C., 1990. Effects of turbulent shear flow on zooplankton distribution. Deep-Sea Research 37, 447–461.

Ho, D.T., Bliven, L.F., Wanninkhof, R., Schlosser, P., 1997. The effect of rain on air–water gas exchange. Tellus 49B, 149–158.

Hobson, E.S., 1966. Visual orientation and feeding in seals and sea lions. Nature 214, 326–327.

Holmes, R.W., Williams, P.M., Eppley, R.W., 1967. Red water in La Jolla Bay, 1964–1966. Limnology and Oceanography 12, 503–512.

Hua, J., Erickson, L.E., Yin, T.Y., Glasgow, L.A., 1993. A review of the effects of shear and interfacial phenomena on cell viability. Critical Reviews in Biotechnology 13, 305–328.

Hyman, M.C., 1990. Numerical simulation of the hydrodynamic wake of a surface ship. Naval Coastal System Center Technical Note, 544–590.

Hyman, M.C., 1992. Simulation of the interaction between a wind-driven sea state and surface ship wakes. Naval Coastal System Center Technical Memorandum, CSS TM 584–591.

Hyman, M.C., 1994. Modeling ship microbubble wakes. Coastal Systems Station Technical Report, CSS/TR-94/39.

Inman, D.L., 1949. Sorting of sediments in the light of fluid mechanics. Journal of Sedimentary Petrology 19, 51–70.

Jimenez, J., 1997. Oceanic turbulence at millimeter scale. Science 61 (Suppl. 1), 47–56.

Juhl, A.R., Velazquez, V., Latz, M.I., 2000. Effect of growth conditions on flow-induced inhibition of population growth of a red-tide dinoflagellate. Limnology and Oceanography 45, 905–915.

Kamykowski, D., Reed, R.E., Kirkpatrick, G.J., 1992. Comparison of sinking velocity, swimming velocity, rotation and path characteristics among six marine dinoflagellate species. Marine Biology 113, 319–328.

Kelly, M.G., 1968. The occurrence of dinoflagellate bioluminescence at Woods Hole. Biological Bulletin 13, 279–295.

Kelly, M.G., Tett, P., 1978. Bioluminescence in the ocean. In: Herring, P.J. (Ed.), Bioluminescence in Action. Academic Press, San Diego, pp. 399–417.

Kimor, B., 1983. Seasonal and bathymetric distribution of thecate and nonthecate dinoflagellates off La Jolla, California. CalCOFI Report 22, 126–134.

Kiørboe, T., Saiz, E., 1995. Planktivorous feeding in calm, and turbulent environments with emphasis on copepods. Marine Ecology Progress Series 122, 135–145.

Kitaigorodskii, S.A., 1997. Effect of breaking of wind-generated waves on the local atmosphere–ocean interaction. Izvestiya, Atmospheric and Ocean Physics 33 (6), 767–774.

Krasnow, R., Dunlap, J., Taylor, W., Hastings, J.W., 1981. Measurements of Gonyaulax bioluminescence, including that of single cells. In: Nealson, K.H. (Ed.), Bioluminescence Current Perspectives. Burgess, Minneapolis, pp. 143–152.

Kunze, E., Sanford, T.B., 1996. Abyssal mixing: where it is not. Journal of Physical Oceanography 26, 2286–2296.

Lapota, D., 1998. Long term and seasonal changes in dinoflagellates bioluminescence in the Southern California Bight. Ph.D. Thesis, University of California, Santa Barbara, 193pp.

Lapota, D., Geiger, M.L., Stiffey, A.V., Rosenberger, D.E., Young, D.K., 1989. Correlations of planktonic bioluminescence with other oceanographic parameters from a Norwegian fjord. Marine Ecology Progress Series 55, 217–227.

Larson, N.G., Gregg, M.C., 1983. Turbulent dissipation and shear in thermohaline intrusions. Nature 306, 26–32.

Latz, M.I., Jeong, H.J., 1996. Effect of red tide dinoflagellate diet and cannibalism on the bioluminescence of the heterotrophic dinoflagellates Protoperidinium spp. Marine Ecology Progress Series 132, 275–285.

Latz, M.I., Lee, A.O., 1995. Spontaneous and stimulated bioluminescence of the dinoflagellate Ceratocorys horrida (Peridiniales). Journal of Phycology 31, 120–132.

Latz, M.I., Rohr, J., 1999. Luminescent response of the red tide dinoflagellate Lingulodinium polyedrum to laminar and turbulent flow. Limnology and Oceanography 44, 1423–1435.

Latz, M.I., Case, J.F., Gran, R.L., 1994. Excitation of bioluminescence by laminar fluid shear associated with simple Couette flow. Limnology and Oceanography 39, 1424–1439.

Laufer, J., 1954. The structure of turbulence in fully developed pipe flow. National Advisory Committee Aeronautical Technical Report No. 1174.

Lazier, J.R.N., Mann, K.H., 1989. Turbulence and the diffusive layers around small organisms. Deep-Sea Research 36, 1721–1733.

Leighton, T.G., 1997. The Acoustic Bubble. Academic Press, San Diego, 613pp.

Lieberman, S.H., Lapota, D., Losee, J.R., Zirino, A., 1987. Planktonic bioluminescence in the surface waters of the Gulf of California. Biological Oceanography 4, 25–46.

Lien, R.C., Gregg, M.C., 2001. Observations of turbulence in a tidal beam and across a coastal ridge. Journal of Geophysical Research 106, 4575–4591.

Losee, J.R., Lapota, D., 1981. Bioluminescence measurements in the Atlantic and Pacific. In: Nealson, K.H. (Ed.), Bioluminescence Current Perspectives. Burgess, Minneapolis, pp. 143–152.

Losee, J.R., Lapota, D., Lieberman, S.H., 1985. Bioluminescence: a new tool for oceanography. In: Zirino, A. (Ed.), Mapping Strategies in Chemical Oceanography. American Chemical Society, Washington, DC, pp. 213–234.

Lovell, J., Kluger, J., 1994. Apollo 13. Pocket Books, New York, 418pp.

Lueck, R.G., Osborn, T., 1986. The dissipation of kinetic energy in a warm-core ring. Journal of Geophysical Research 91 (C1), 803–818.

Lueck, R.G., Crawford, W.R., Osborn, T.R., 1983. Turbulent dissipation over the continental slope off Vancouver Island. Journal of Physical Oceanography 13, 1809–1818.

Lynch, D.K., Livingston, W., 1995. Color and Light in Nature. University Press, Cambridge, 254pp.

Lythgoe, J.N., 1972. The adaptation of visual pigments to the photic environment. In: Dartnall, H.J.A. (Ed.), Handbook of Sensory Physiology, Vol. VII. Springer, New York, pp. 566–603.

Mann, K.H., Lazier, J.R.N., 1996. Dynamics of marine ecosystems biological–physical interactions in the ocean. Blackwell Sciences Inc., London, 394pp.

Manton, M.J., 1973. On the attenuation of sea waves by rain. Geophysical Fluid Dynamics 5, 249–260.

Mead, K.S., Denny, M.W., 1995. The effects of hydrodynamic shear stress on fertilization and early development of the purple sea urchin *Strongylocentrotus purpuratus*. Biological Bulletin 188, 46–56.

Medwin, H., Clay, C.S., 1998. Fundamentals of Acoustic Oceanography. Academic Press, San Diego, 712pp.

Medwin, H., Daniel Jr., A.C., 1990. Acoustic measurements of bubble production by spilling breakers. Journal of Acoustical Society of America 88, 404–412.

Mehta, A.J., Parchure, T.M., Dixit, J.G., Ariathuri, R., 1982. Resuspension potential of deposited cohesive beds. In: Kennedy, V.S. (Ed.), Estuarine Comparisons. Academic Press, New York, pp. 591–609.

Mensinger, A.F., Case, J.F., 1992. Dinoflagellate luminescence increases susceptibility of zooplankton to teleost predation. Marine Biology 112, 207–210.

Miller, M.C., McCave, Komar, P.D., 1977. Threshold of sediment motion under unidirectional currents. Sedimentology 24, 507–527.

Morin, J.G., 1983. Coastal bioluminescence: patterns and functions. Bulletin of Marine Science 33, 787–817.

Nauen, J.C., 1998. Biomechanics of two aquatic defense systems. Ph.D. Thesis, University of California, San Diego, 159pp.

Oakey, N.S., Elliot, J.A., 1980. Dissipation in the mixed layer near Emerald Basin. In: Nihoul, J.C.J. (Ed.), Marine Turbulence. Elsevier, Amsterdam, pp. 123–133.

Oakey, N.S., Elliot, J.A., 1982. Dissipation within the surface mixed layer. Journal of Geophysical Research 12, 171–185.

Osborn, T.R., 1980. Estimates of the local rate of vertical diffusion from dissipation measurements. Journal of Physical Oceanography 10, 83–89.

Phillips, O.J., 1980. The Dynamics of the Upper Ocean. Cambridge University Press, Cambridge, 336pp.

Pond, S., Pickard, G.L., 1983. Introductory Dynamical Oceanography, 2nd Edition. Pergamon Press, New York, 329pp.

Pumphrey, H.C., Crum, L.A., Bjorno, L., 1989. Underwater sound produced by individual drop impacts. Journal of the Acoustical Society of America 85, 1518–1526.

Rapoport, H.S., Latz, M.I., 1998. In situ bioluminescence measurements from the Scripps Pier, La Jolla, CA. EOS, American Geophysical Union 79 (1), OS25.

Richardson, W.J., Greene, C.R., Malme, C.I., Thomson, D.H., 1995. Marine Mammals and Noise. Academic Press, New York, 576pp.

Robinson, K., 1998. Dolphins glow in bioluminescent sea. Biophotonics International, September/October 1987.

Rohr, J.J., Losee, J.R., Hoyt, J.W., 1990. Stimulation of bioluminescence by turbulent pipe flow. Deep-Sea Research 37, 1639–1646.

Rohr, J., Losee, J., Anderson, G., 1994. The response of bioluminescent organisms to fully developed pipe flow. Naval Command, Control and Ocean Surveillance Center, RDT&E Division. Technical Report 1360.

Rohr, J., Allen, J., Losee, J., Latz, M.I., 1997. The use of bioluminescence as a flow diagnostic. Physics Letters A 228, 408–416.

Rohr, J., Latz, M.I., Fallon, S., Nauen, J.C., Hendricks, E., 1998. Experimental approaches towards interpreting dolphin-stimulated bioluminescence. Journal of Experimental Biology 201, 1447–1460.

Roithmayr, C.M., 1970. Airborne low-light sensor detects luminescing fish schools at night. Commercial Fishery Review 32, 42–51.

Rood, E.P., 1995. The emergence of computational ship hydrodynamics. Naval Research Reviews XLVII, 8–18.

Rosenhead, L., 1963. Laminar Boundary Layers. Dover Publications, New York, 687pp.

Rothschild, B.J., Osborn, T.R., 1988. Small-scale turbulence and plankton contact rates. Journal of Plankton Research 10, 465–474.

Sandstrom, H., Oakey, N.S., 1995. Dissipation in internal tides and solitary waves. Journal of Physical Oceanography 25, 604–614.

Sanford, L.P., 1993. Wave forced erosion of bottom sediment in Chesapeake Bay. Estuaries 17 (1B), 148–165.

Schlichting, H., 1979. Boundary-layer theory. McGraw-Hill, New York, 814pp.

Seim, H.E., Gregg, M.C., 1997. The importance of aspiration and channel curvature in producing strong vertical mixing over a sill. Journal of Geophysical Research 102 (C2), 3451–3472.

Seim, H.E., Winkel, D.P., Gawarkiewicz, G., Gregg, M.C., 1999. A benthic front in the Straits of Florida and its relationship to the structure of the Florida current. Journal of Physical Oceanography 29, 3125–3132.

Seliger, H.H., Fastie, W.G., McElroy, W.D., 1961. Bioluminescence in the Chesapeake Bay. Science 133, 699–700.

Seliger, H.H., Fastie, W.G., McElroy, W.D., 1969. Towable photometer for rapid area mapping of concentrations of bioluminescence marine dinoflagellates. Limnology and Oceanography 14, 806–813.

Seliger, H.H., Carpenter, J.H., Loftus, M., McElroy, W.D., 1970. Mechanisms for the accumulation of high concentrations of dinoflagellates. Limnology and Oceanography 15, 234–245.

Shaw, W.C., 1959. Sea Animals and Torpedoes. US Naval Ordinance Test Station, Report 6573, 44pp.

Shay, T.J., Gregg, M.C., 1984. Turbulence in an oceanic convective mixed layer. Nature 310, 282–285.

Sherman, F., 1990. Viscous Flow. McGraw-Hill, New York, 746pp.

Soloviev, A.V., Vershinsky, N.V., Bezverchnii, V.A., 1988. Small-scale turbulence measurements in the thin surface layer of the ocean. Deep-Sea Research 35, 1859–1874.

Stacey, M.T., Monismith, S.G., Burau, J.R., 1999a. Observations of turbulence in a partially stratified estuary. Journal of Physical Oceanography 29, 1950–1970.

Stacey, M.T., Monismith, S.G., Burau, J.R., 1999b. Measurements of Reynolds stress profiles in unstratified tidal flow. Journal of Geophysical Research 104 (C5), 1093–10949.

Staples, R.F., 1966. The distribution and characteristics of surface bioluminescence in the oceans. Naval Oceanographic Office Technology Report TR-184, pp. 1–48.

Sternberg, R.W., 1968. Friction factors in tidal channels with differing bed roughness. Marine Geology 6, 243–260.

Sullivan, J.M., Swift, E., 1994. Photoinhibition of mechanically stimulated bioluminescence in the autotrophic dinoflagellate, Ceratium fusus (Pyrrophyta). Journal of Phycology 30, 637–643.

Sullivan, J.M., Swift, E., 1995. Photoenhancement of bioluminescence capacity in natural and laboratory populations of the autotrophic dinoflagellate Ceratium fusus (Ehrenb.) Dujardin. Journal of Geophysical Research 100 (C4), 6565–6574.

Swean, T., 1987. Numerical simulations of the wake downstream of a twin screw destroyer model. Naval Research Laboratory Memorandum Report 6131, December.

Sweeney, B.M., 1963. Bioluminescent dinoflagellates. Biological Bulletin 125, 177–181.

Sweeney, B.M., 1981. Variations in the bioluminescence per cell in dinoflagellates. In: Nealson, K.H. (Ed.), Bioluminescence: Current Perspectives. Burgess, Minneapolis, pp. 90–94.

Sweeney, B.M., Haxo, F.T., Hastings, J.W., 1959. Action spectra for two effects of light on luminescence in Gonyaulax polyedra. Journal of General Physiology 43, 285–299.

Swift, E., Meunier, V.A., Biggley, W.H., Hoarau, J., Barras, H., 1981. Factors affecting bioluminescent capacity in oceanic dinoflagellates. In: Nealson, K.H. (Ed.), Bioluminescence: Current Perspectives. Burgess, Minneapolis, pp. 95–106.

Swift, E., Sullivan, J.M., Batchelder, H.P., Van Keuren, J., Vaillancourt, R.D., 1995. Bioluminescent organisms and bioluminescence measurements in the North Atlantic Ocean near latitude 59.5°N, longitude 21°W. Journal of Geophysical Research 100 (C4), 6527–6547.

Tarasov, N.I., 1956. Luminescence of the sea (Svechenie Moria) Moscow, Akadamie Nauk SSSR. Institute Oceanologii. Trans. M. Slessers., 1957. US Naval Oceanographic Office Report No. NOOT-21.

Tavolga, T., 1967. Noisy chorus of the sea. Natural History 76, 20–27.

Tennekes, H., Lumley, J.L., 1972. A First Course in Turbulence. The MIT Press, Cambridge, MA, 300pp.

Terray, E.A., Donelan, M.A., Agrawal, Y.C., Drennan, W.M., Kahma, K.K., Williams III, A.J., Hwang, P.A., Kitaigorodskii, S.A., 1996. Estimates of kinetic energy dissipation under breaking waves. Journal of Physical Oceanography 26, 792–799.

Thomas, W.H., Gibson, C.H., 1990a. Quantified small-scale turbulence inhibits a red tide dinoflagellate, Gonyaulax polyedra Stein. Deep-Sea Research 37, 1583–1593.

Thomas, W.H., Gibson, C.H., 1990b. Effects of small-scale turbulence on microalgae. Journal of Applied Phycology 2, 71–77.

Thomas, W.H., Gibson, C.H., 1992. Effects of quantified small-scale turbulence on the dinoflagellates, Gymnodinium sanguineum (splendens): contrasts with gonyaulax (lingulodinium) polyedra, and the fishery implication. Deep-Sea Research 39, 1429–1437.

Tritton, T., 1988. Physical Fluid Dynamics, 2nd Edition. Oxford University Press, New York, 519pp.

Turner, R.J., 1965. Notes on the nature and occurrence of marine bioluminescence phenomena. National Institute of Oceanography Internal Report No. B4, July 1965, Wormley, Godalming, Surrey.

Tynan, C., 1993. The effects of small-scale turbulence on dinoflagellates. Ph.D. Thesis, University of California, San Diego, 227pp.

Vasil'kov, A.V., Yefimov, S.V., Kondranin, T.V., 1992. Remote measurements of bioluminescence in the sea. Oceanology 32, 530–533.

Veron, F., Melville, W.K., 1999. Pulse-to-pulse coherent doppler measurements of waves and turbulence. Journal of Atmospheric and Oceanic Technology 16, 1580–1597.

Widder, E.A., Case, J.F., 1981. Bioluminescence excitation in a dinoflagellate. In: Nealson, K.H. (Ed.), Bioluminescence: Current Perspectives. Burgess, Minneapolis, pp. 125–132.

Widder, E.A., 1997. Bioluminescence—shedding light on plankton distribution patterns; evolution of instrumentation; underutilized oceanographic tool. Sea Technology March, 33–39.

Widder, E.A., Bernstein, S.A., Bracher, D.F., Case, J.F., Reisenbichler, K.R., Torres, J.J., Robison, B.H., 1989. Bioluminescence in Monterey Submarine Canyon: image analysis of video recordings from a midwater submersible. Marine Biology 100, 541–551.

Widder, E.A., Case, J.F., Bernstein, S.A., MacIntyre, S., Lowenstine, M.R., Bowlby, M.R., Cook, D.P., 1993. A new large volume bioluminescence bathyphotometer with defined turbulence excitation. Deep-Sea Research I 40, 607–627.

Williams, T.M., Kooyman, G.L., 1985. Swimming performance and hydrodynamic characteristics of harbor seals *Poca vitulina*. Physiology Zoology 58, 576–589.

Wyatt, T., 1987. They moved in tracks of shining white. Journal du Conseil 44, 56–58.

Yamazaki, H., Lueck, R.L., 1990. Why dissipation rates are not lognormal. Journal of Physical Ocenography 20, 1907–1918.

Yamazaki, H., Osborn, T.R., 1988. Review of oceanic turbulence: implications for biohydrodynamics. In: Rothschild, B.J. (Ed.), Toward a Theory on Biological–Physical Interactions in the World Ocean. Kluwer Academic Publishers, Boston, pp. 215–234.

Zirbel, M.J., Veron, F., Latz, M.I., 2000. The reversible effect of flow on the morphology of *Ceratocorys horrida* (Peridiniales, Dinophyta). Journal of Phycology 36, 46–58.